1 2.

FINAL REPORT

INVESTIGATION OF ELECTRODE MATERIALS FOR ALKALINE BATTERIES

JPL 952265

This work was performed for the Jet Propulsion Laboratory, California Institute of Technology, sponsored by the National Aeronautics and Space Administration under Contract NAS7-100.

G. Myron Arcand

Department of Chemistry

Idaho State University

Pocatello, Idaho

15 November 1971

NOTICE

This report was prepared as an account of Government-sponsored work. Neither the United States, nor the National Aeronautics and Space Administration (NASA), nor any person acting on behalf of NASA:

a. Makes warranty or representation, expressed or implied, with respect to the accuracy, completeness, or usefulness of the information contained in this report, or that the use of any information, apparatus, method, or process disclosed in this report may not infringe privately-owned rights; or

b. Assumes any liabilities with respect to the use of, or for damages resulting from the use of any information, apparatus, method or process disclosed in this report.

As used above, "persons acting on behalf of NASA" includes any employee or contractor of NASA, or employee of such contractor, to the extent that such employees or contractor of NASA, or employee of such contractor prepares, disseminates, or provides access to, any information pursuant to his employment with such contractor.

Requests for copies of this report should be referred to:

National Aeronautics and Space Administration
Office of Scientific and Technical Information
Washington 25, D.C.

Attention: AFSS-A

TABLE OF CONTENTS

LIST OF TABLES

LIST OF FIGURES

ABSTRACT

The objectives of the contract are four-fold:

(1) Study of the amalgam electrode.

(2) Study of the reduction of Ag(I) by zinc.

(3) Study of the evolution of gas at electrodes.

(4) Study of the thermal decomposition of Ag_2O and AgO.

The study of rechargeable amalgam electrodes comprises a major part of the work performed under this contract.

Various amalgam electrodes have been investigated for possible use as high-rate anodes and cathodes. The K(Hg) and Na(Hg) anodes in 10 VF* and 15 VF hydroxide solutions have proven satisfactory; some of these have produced current-densities of more than 8 A/cm^2. None of the amalgam cathodes have approached this performance although the Tl(Hg) has delivered 1 A/cm^2. Se(Hg) and Te(Hg) cathodes have given very stable discharges.

Zn(Hg) and Cd(Hg) electrodes did not show good high-rate characteristics, 200-300 mA/cm^2 being about the maximum current-densities obtainable. Both anodes are charged through a two-step process in which M(Hg) is first formed electrochemically and subsequently reduces Zn(II or Cd(II) to form the corresponding amalgam. The second step is extremely rapid for zinc and very slow for cadmium.

---

*The symbol, VF, is used as an unambiguous expression of concentration and indicates the number of formula-weights of solute dissolved in a liter of solution. It is distinguished from the symbol, WF, the unit expressing the number of formula-weights of solute dissolved in one kilogram of solvent. The symbol is accepted in papers published in the Journal of the American Chemical Society and in Analytical Chemistry.

Both K(Hg) and Na(Hg) electrodes have a fairly short stand-life in 10 VF hydroxide. Recovery was generally less than 50% after a stand of 15 days. On the other hand, a K(Hg) electrode in saturated KOH showed a charge-recovery of 85% after 0.7 year. Unfortunately, the saturated-electrolyte electrodes are quite noisy during high-rate discharge.

Several combinations of K(Hg) and Na(Hg) anodes with Ag/AgO and Ni-NiOOH cathodes have been assembled into cells and batteries. A single K(Hg) - Ag/AgO cell has produced a "short-circuit" peak current as high as 240 A. This corresponds to nominal current-densities of at least 3.6 A/cm^2. A 6-cell battery delivered 10.8 V at 10.8 A into a 1-ohm load. A 5-cell battery (one cell shorted out) delivered a peak current of 320 A for 0.5 second.

A two-electrode button cell produced a peak of 3 A at 0.5 V on "short-circuit"; the current decreased to 0.5 A in 30 seconds. The relatively high voltage was probably caused by high cell-resistance.

Non-aqueous solvents have not been satisfactory since electrolyte ionization and/or solubility is too low to allow the high currents desired.

The amalgam batteries show great promise as special-purpose devices which can deliver high currents from small packages. Further work on an engineering scale is needed to develop them into useful primary and/or secondary batteries. Containment of the amalgam, suppression of gassing, and development of adequate separators are some of the problems in need of solution.

As part of the study of the reduction of Ag(I) by zinc, the solubility of Ag_2O in 10 VF KOH was estimated by a tracer method to be 3.5×10^{-4} VF (measured as the concentration of Ag(I)). This compares favorably with the 4×10^{-4} VF found polarographically.

More than 90% of Ag(I) in KOH is removed from the solution within five hours if zinc metal is present. Deposited silver permanently decreases the effective surface area of a zinc anode by about 15%. The electrode can be rejuvenated by vigorously generating gas on it after the silver deposition has ceased.

The approximate composite diffusion coefficient for the Ag(I) species in 10 VF KOH is 2.75×10^{-6} $cm^2 sec^{-1}$. Not surprisingly, this value suggests a relatively large diffusing particle in this system.

An additional area of work included in this contract concerns the evolution of gas at electrodes. Much work has yet to be done on the hydrogen polarization on zinc in concentrated KOH solutions. First indications are that the extrapolated exchange current-density is 10-20μA/cm^2 in 0.1 VF KOH, 50-75μA/cm^2 in 1 VF KOH, and 150-250μA/cm^2 in 10 VF KOH. For cadmium in 10 VF KOH, the value is about 12 mA/cm^2. The results indicate a decreasing hydrogen overpotential with increasing KOH concentration which appears to follow a square-root relationship.

Studies of the thermal decomposition of AgO and Ag_2O were also a part of this effort.

The activation energy for the decomposition of Ames Chemical Works AgO has been estimated at 26.2 kcal/mole and that of Ag_2O at 43 kcal/mole.

Ag_2O apparently begins to decompose at 260°, a temperature considerably lower than the usually reported decomposition temperature. The rate of decomposition increases with time at these temperatures.

If AgO is heated in a laboratory atmosphere at a temperature between 60° and 100°, the substance regains enough weight to raise the final total above the initial value when it is allowed to stand at room temperature for a period of time. Heating-cooling cycles increase the effect. No such effect has been observed below 60°.

Effects are different in other atmospheres. When AgO is heated in vacuum, cooled, and exposed to air, no weight-gain is observed. Similarly, no gain is observed if the sample is heated and cooled in dry nitrogen. Similar behavior is observed in oxygen as long as oxygen is flowing in the system; the weight begins to increase immediately whenever the gas flow is stopped. When a sample is heated and cooled in dry air, the observed changes are smaller than those observed in laboratory air. Apparently, heating AgO activates it so that it can adsorb material, water or oxygen, from the atmosphere. It is probable that one of the substances acts as a catalyst for the adsorption of the other.

The objectives of the contract are four-fold:

(1) Study of the amalgam electrode.

(2) Study of the reduction of Ag(I) by zinc.

(3) Study of the evolution of gas at electrodes.

(4) Study of the thermal decomposition of Ag_2O and AgO.

A. AMALGAM ELECTRODES

Introduction

The fortuitous observation and crude early experiments which led to a full-scale investigation of amalgam electrodes have been described[1]. Amalgamated zinc electrodes are commonly used in battery construction to prevent self-discharge as in the silver-zinc cell or the Ruben mercury cell. Only a few instances are on record in which a liquid amalgam containing the dissolved active element is used as a voltaic-cell electrode. A patent has been issued to Mallory Batteries Ltd. for a regenerative cell employing a liquid zinc-amalgam anode, but no performance data are available[2]. Le Duc, et al[3] report the use of a sodium-amalgam anode in a fuel cell. Lica[4] reports the production of rechargeable batteries very similar to the ones described below. It must be presumed that certain aspects of Lica's work and that done here overlap; however, details and results of his work are not readily available.

Exploratory work in this laboratory involved testing a number of metal-amalgam combinations both as potential rechargeable anodes and as cathodes. The capability of delivering very high current-densities was the primary characteristic sought. None of the cathodes were satisfactory in this respect, but the potassium-amalgam, K(Hg), and the sodium-amalgam, Na(Hg), showed real promise as anodes. The zinc-amalgam, Zn(Hg), is a possibility for some limited applications.

Stand-life characteristics of K(Hg), Na(Hg), and Zn(Hg) electrodes were investigated in various KOH solutions. The fairly poor results led to a search for non-aqueous solvents which might be satisfactory.

Various laboratory cells and batteries ranging from "button" size to multicell batteries about 15 cm long were produced. Since amalgam cathodes showed no advantage over conventional cathodes, AgO and NiOOH cathodes were used. These units were built to deliver very high currents and, in some cases, were successful.

Experimental

Reagents

Mercury was purified by drawing air through the liquid for several hours, pinholing the metal into dilute HNO_3, and triply distilling the product. Unless otherwise indicated, all chemicals were J. T. Baker Reagent Grade. KOH was obtained both as 45% solutions and as pellets; all other hydroxides were in solid form. Silver powder was obtained from Ames Chemical Works and from Handy and Harmon. Solid electrode supports were expanded-silver grid (5 Ag 7-4/0, Exmet Corp.). TlOH was obtained from Alfa, Ventron Corp. Chemical Division.

Most of the separator materials used were obtained from Jet Propulsion Laboratory as were all NiOOH electrodes. MBS-1 and MBS-2 separators were obtained from Membrionics Corp. Epoxy cement used for separator mounting was Kontes K-25090.

Equipment

Constant currents were supplied by an Electronics Measurements Model C629CMK power supply. Potentials were followed with a Dohrmann Model RSC1100 multi-range recorder, a Honeywell Model Y143X(58) 1-mV recorder coupled with a Cahn #1490 recorder controller, or a Texas Instruments Servo/Riter Model II recorder. Currents up to 10 A were measured with an

RCA VOM Model WV-3A; higher currents were measured with a properly shunted Westinghouse ammeter. Current transients were measured with a Tektronix Model 564B storage oscilloscope equipped with a Model 3A9 vertical amplifier and a Model 2B67 time base.

Open-circuit electrode potentials were measured with a Leeds and Northrup K-3 potentiometer with a Leeds and Northrup Model 2430-C guarded galvanometer. Part of the test-cell potential was balanced with an Eppley Student's standard cell. The cell container was a Kontes K-25005 Amalgam Electrode Holder. The reference electrode was an Electrochemical Research Associates Hg/HgO electrode.

Procedures

Single electrodes were studied using pool amalgams or hanging-drop amalgams. All potentials were measured against Hg/HgO references and are so reported.

A typical cup cell is shown in Figure 1. The electrolyte concentration was the same throughout the system. The Luggin capillary was positioned within a few millimeters of the amalgam surface. The anode surface area was determined from the diameter of the cup. This type of cell was used for relatively low current-densities, usually not more than 1 A/cm^2. The electrolyte solution contained the hydroxide of the active metal. Amalgams were charged at a convenient current-density; discharges were at various rates with completion taken as the point where the measured voltage was half the open-circuit voltage (OCV).

The hanging-drop assembly is shown schematically in Figure 2. The container was a 400-ml beaker with the top cut off and covered with a Teflon cap with holes drilled for the various components. The hanging-drop electrode was located in the center. The auxiliary electrode was a platinum mesh cylinder about 4 cm in diameter. Drop size was measured by collecting ten drops of mercury from the dropping-mercury electrode (DME),

washing, drying, and weighing. The area of each drop was calculated, assuming that the drops were identical and that no change in size occurred with amalgamation. The mercury drop was transferred to the working electrode by collecting it from the DME in the drop cup and attaching it to the platinum contact of the drop holder. The tip of the Luggin capillary was positioned as close as possible to the drop.

Drop electrodes were charged and discharged in the usual manner, the behavior being followed with an oscilloscope. At the highest rates, discharge times were less than one second.

Stand-life experiments were made by charging a number of amalgam electrodes equally and allowing them to stand for varying lengths of time before discharge. The cells each contained the same amount of mercury and identical electrolyte solutions. They were connected in series to the constant-current power supply and charged at a fixed rate. When charging was discontinued, the amalgams were transferred into test tubes containing appropriate electrolyte solutions. These were stoppered and set aside for different periods. Each was discharged at a rate known to be efficient and the relative recovery was determined.

Electrode OCV measurements were made on an amalgam pool containing 2.2 g of mercury. Nitrogen was passed through a bubbler train containing vanadous solution[5] to remove oxygen and then into the cell. The cell was allowed to reach temperature equilibrium in a water bath set at 24.6° before the amalgam was charged. The counter electrode for the charging process was a platinum wire mounted in the side-arm containing the nitrogen inlet.

Various configurations were tried for preparing galvanic cells and batteries. Only the relatively successful designs will be described.

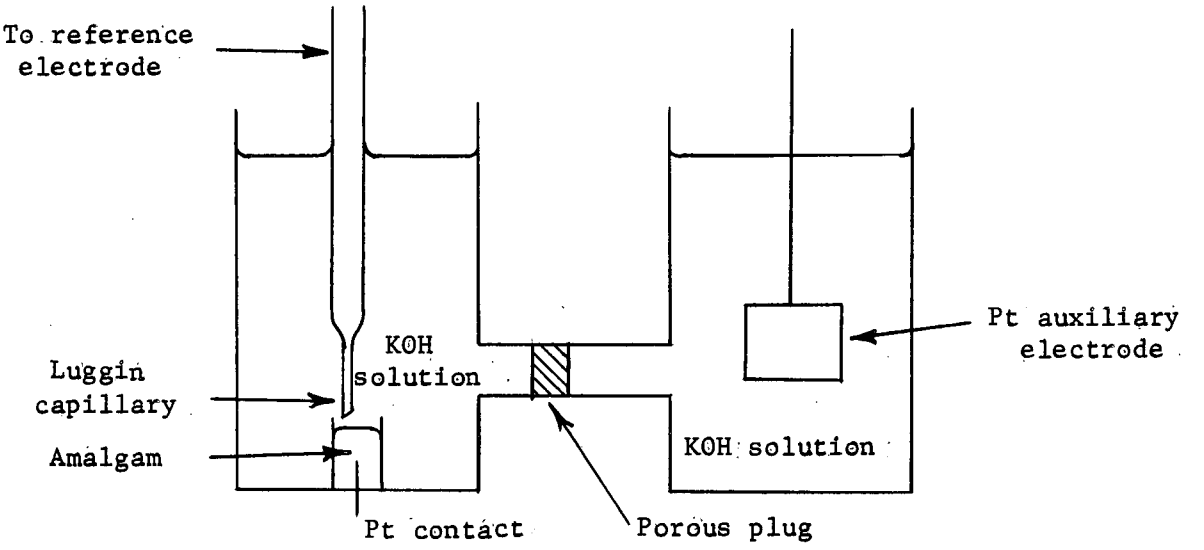

Figure 1. Cup Cell for Amalgam-Electrode

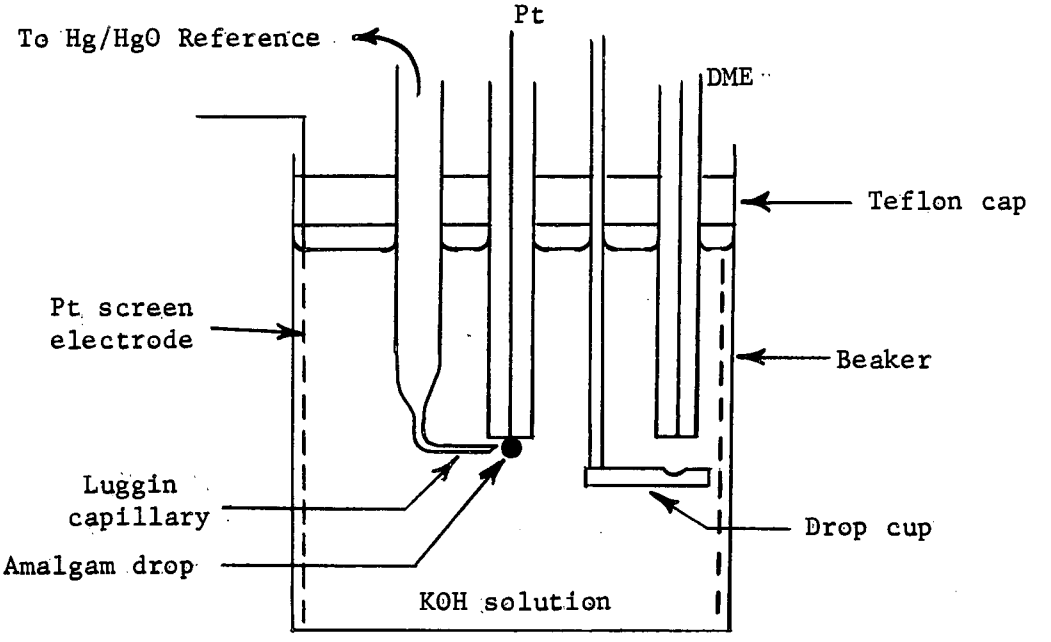

Figure 2. Cell for Hanging-Drop Electrode

Figure 3 shows a schematic design of a rectangular container which allowed fabrication of cells and batteries with various numbers of electrodes and cells. The container was made of 1/8" sheets of Plexiglas bonded together with epoxy cement. The side sections had 1/16" grooves into which electrodes or separator supports could be fastened temporarily. The separator supports were made of a thin ceramic material cut as shown. The supports were usually fastened in position with paraffin. Various separator materials and combinations were cemented to the supports as required. Where multi-cell batteries were made, ceramic or Plexiglas insulators were placed in the appropriate slots. Electrodes were interconnected with cables woven from several lengths of #12 copper wire. Silver electrodes were made by pressing 3-micron silver powder onto expanded-silver grid and sintering in air at 700°. Nickel electrodes used were commercial types obtained from JPL. Copper leads were cadmium-soldered to the solid electrodes.

Most charging was done at constant current. Some was done at constant voltage using the constant-voltage control procedure available with the C629CMK power supply. Where constant voltage was used, chemical coulometers[6,7] were used to measure the charge.

A button-sized cell was fabricated as shown in Figure 4. The outer shell was a 5-mm piece of 12-mm O.D. polyethylene tubing. A piece of sheet copper was cemented to the end of the tube. The inner section was a 2-mm piece of 8-mm O.D. polyethylene tubing with a layer of cellophane separator cemented over the end. The AgO electrode was a circle 8 mm in diameter. The amalgam was charged externally and a small amount was added to the cell. A drop of KOH solution was added and the inner section was inserted so that the separator was in the solution. A small hole was punched in the cellophane to allow escape of gas. The AgO electrode (pre-charged) was then

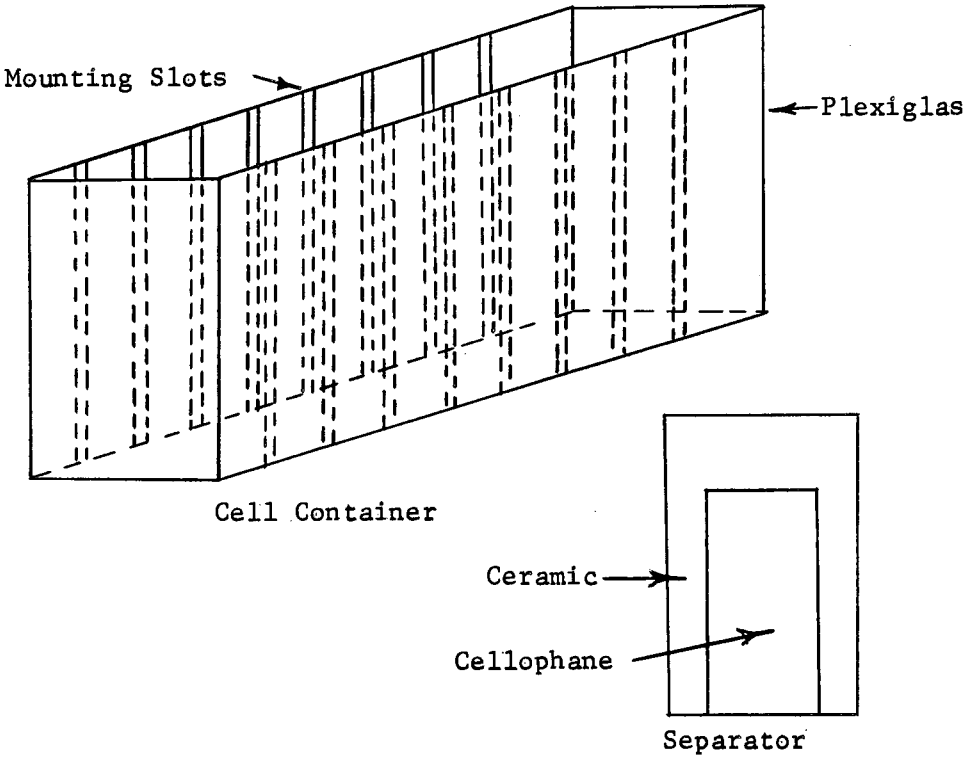

Figure 3. "Universal" Battery Case

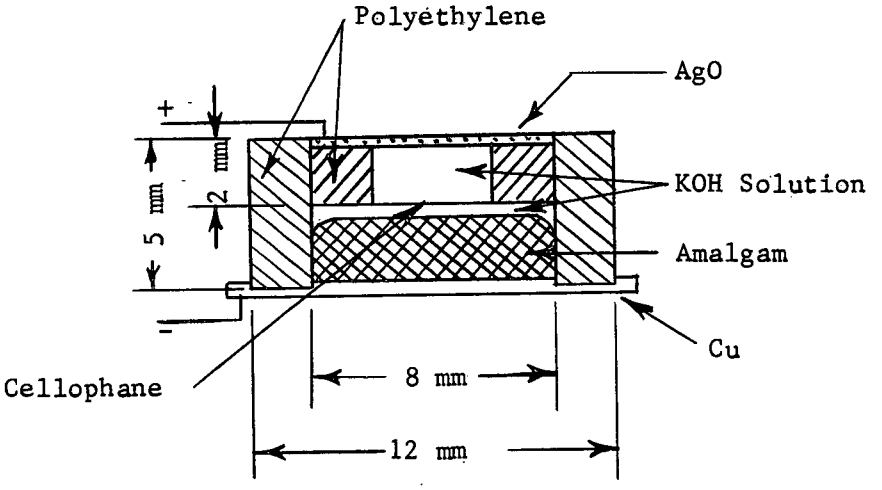

Figure 4. K(Hg) - Ag/AgO Button Cell

placed on top of the inner section and two drops of KOH solution were added. Leads were #12 copper wire cadmium-soldered to the copper sheet and to the silver grid.

Results and Discussion

A number of possible amalgam systems was surveyed: lithium, sodium, and potassium in Group I, magnesium, calcium, and barium in Group II, aluminum in Group III, lead in Group IV, copper in Group Ib, and zinc and cadmium in Group IIb. Of these, sodium and potassium appeared satisfactory for producing high-rate, secondary electrodes. All of the others have relatively insoluble hydroxides. Self-discharge of the active-metal amalgams is inhibited by high base concentration (or low water activity) and the high hydroxide concentration had to be obtained by adding NaOH or KOH. In all cases studied, the added alkali metal became the active substance during charge; e.g., if a mixture of Cd(II) and KOH were electrolyzed, K(Hg) would form rather than Cd(Hg).

The discharge behavior of an amalgam electrode which was charged in the presence of Cd(II) and 10 VF KOH is shown in Figure 5. The notable characteristic is the very negative working potential which is not more positive than -1.4 V vs Hg/HgO at 535 mA/cm^2 until discharge is almost complete. When cadmium metal is dissolved directly in mercury and the electrode potential measured in 10 VF KOH, the OCV is about -0.78 V vs Hg/HgO while a solid cadmium electrode in a similar solution shows an OCV of about -0.88 V. Thus, the electrode charged electrolytically does not behave at all like an ordinary cadmium or cadmium-amalgam electrode.

Figure 6 shows the results of an experiment where a "cadmium-amalgam" electrode was charged for one-minute intervals interspersed with one-minute intervals on open circuit. The charge potentials were all uniformly high and relatively steady. However, the initial OCV values were around -0.8 V vs Hg/HgO as expected for a Cd(Hg) electrode, but after a time, a sharp

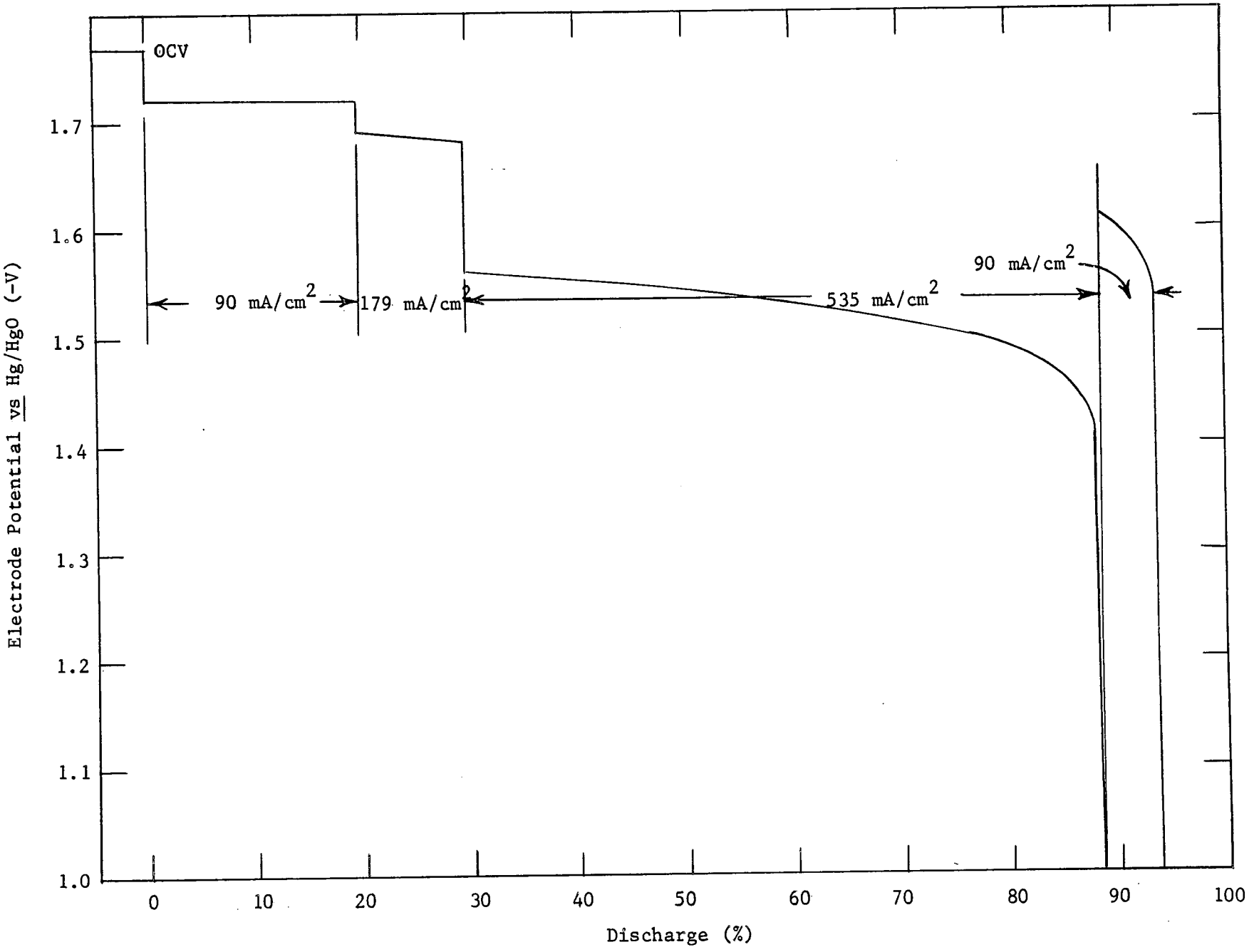

Figure 5. Discharge of Cd(Hg) Electrode in 10 VF KOH

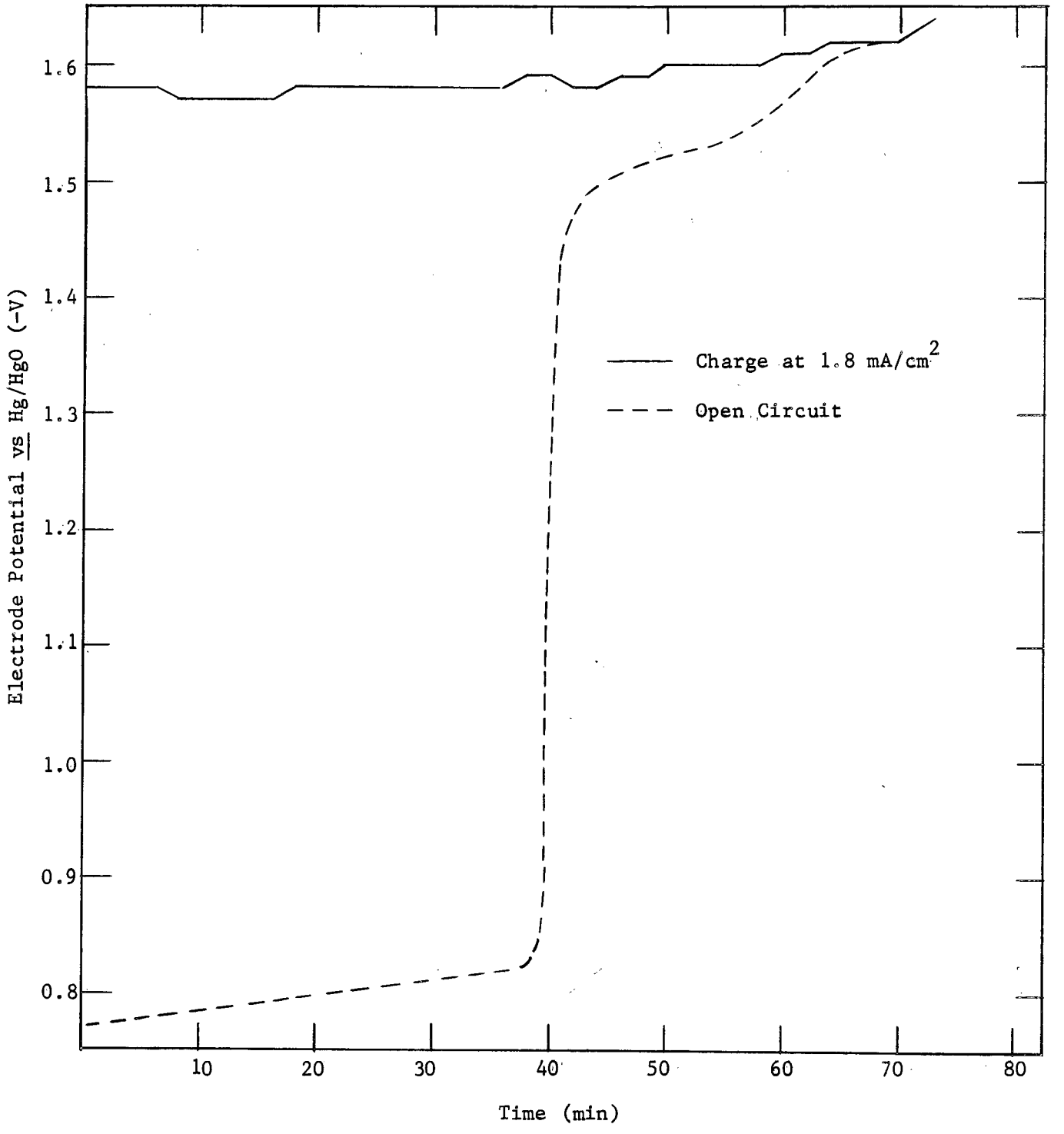

Figure 6. Alternate Open-Circuit-Charge Behavior of the Cd(Hg) Electrode

break is noted and the higher OCV is seen.

One would normally expect Cd(II) to be more easily reduced than K(I). The charge potential observed in Figure 6 indicates that this is not true in this system. Still, one would expect K(Hg) to reduce Cd(II) to produce Cd(Hg). Something of this sort apparently occurs at very low charge rates and while total charge is also low so that there appears to be Cd(Hg)/CdO control. However, as charge builds, the K(Hg) seems to lose the ability to further reduce Cd(II) and the amalgam potential rises to a value closer to that of the K(Hg). It is possible that a CdO layer slowly forms on the amalgam surface which tends to prevent access to Cd(II) in solution and which is, itself, not readily reduced. At the same time, K(I) apparently can reach the metal surface.

When the "cadmium-amalgam" is charged very slowly and then discharged shortly after the OCV and the charge potentials coincide, recovery is found to be very poor. This suggests that most of the potassium is re-oxidized during the very slow charge. If charge is carried on well past the coincidence point, reasonable recovery (>75%) is possible. When the electrode is charged without interruption at higher rates, the opportunity for re-oxidation is less and good recovery is obtained. However, the electrode behaves as a K(Hg), not a Cd(Hg), electrode.

The other metals mentioned were not studied as extensively as Cd; however, their general charge and discharge behaviors indicate that similar phenomena are occurring. The exception is zinc.

The Zn(Hg) electrode was of interest because it should have a very long stand life and, although it would produce cells of lower voltage than the alkali metals, the stand characteristic coupled with high discharge rate would be useful.

Figure 7 shows a typical discharge for a Zn(Hg) electrode. The characteristics are quite satisfactory at this current-density. Furthermore, this electrode can be charged with high efficiency at rates as high as 5 A/cm^2. However, further experiments showed the maximum discharge rate to be 200 - 300 mA/cm^2. An attempt to use this electrode as a cathode in conjunction with a K(Hg) anode showed that the maximum rate of direct reduction of Zn(II) into the amalgam was 200 - 300 mA/cm^2. Thus, the high charge rate is evidently the result of a two-step process in which K(Hg) is formed which then rapidly and stoichiometrically reduces Zn(II) to form the Zn(Hg).

The Zn(Hg) anode may still have some value. It has a long stand-life, has discharge characteristics comparable with its porous counterpart, does not form dendrites, does not slough, and can be charged at a very high rate.

Because a fairly short stand-life was expected in aqueous solutions, some non-aqueous solvents were investigated. Propylene carbonate (PC) showed little promise; $KHCO_3$, KOH, KCl, and $KHC_8H_4O_4$ are only slightly soluble in PC while maximum current-densities obtainable were less than 100$\mu A/cm^2$. Alkali-metal perchlorates are more soluble in PC, but electrodes produced current-densities of 5 mA/cm^2 and less.

Dimethyl formamide (DMF) is little better. A complete cell consisting of a Li(Hg)/$LiClO_4$ - DMF anode and a Cu(Hg)/$CuCl_2 \cdot 2H_2O$ - DMF cathode accepted a charge of 2.5 mA-hr and produced an OCV of 2.25 V. Its maximum discharge rate was 2 mA with 60% recovery.

A K(Hg)/10 VF KOH//$CuCl_2$-DMF/Cu(plate) cell was charged at 50 mA for six minutes at which time the OCV was 2.13 V. The cathode plate area was 46 cm^2. The cell was discharged through a decade resistor. At R = 0, I = 20 mA; at R = 140 ohms, I = 10 mA and E = 1.1 V. The voltage held essentially constant for 35 minutes when it dropped abruptly to 0.5 V. Charge recover was virtually complete.

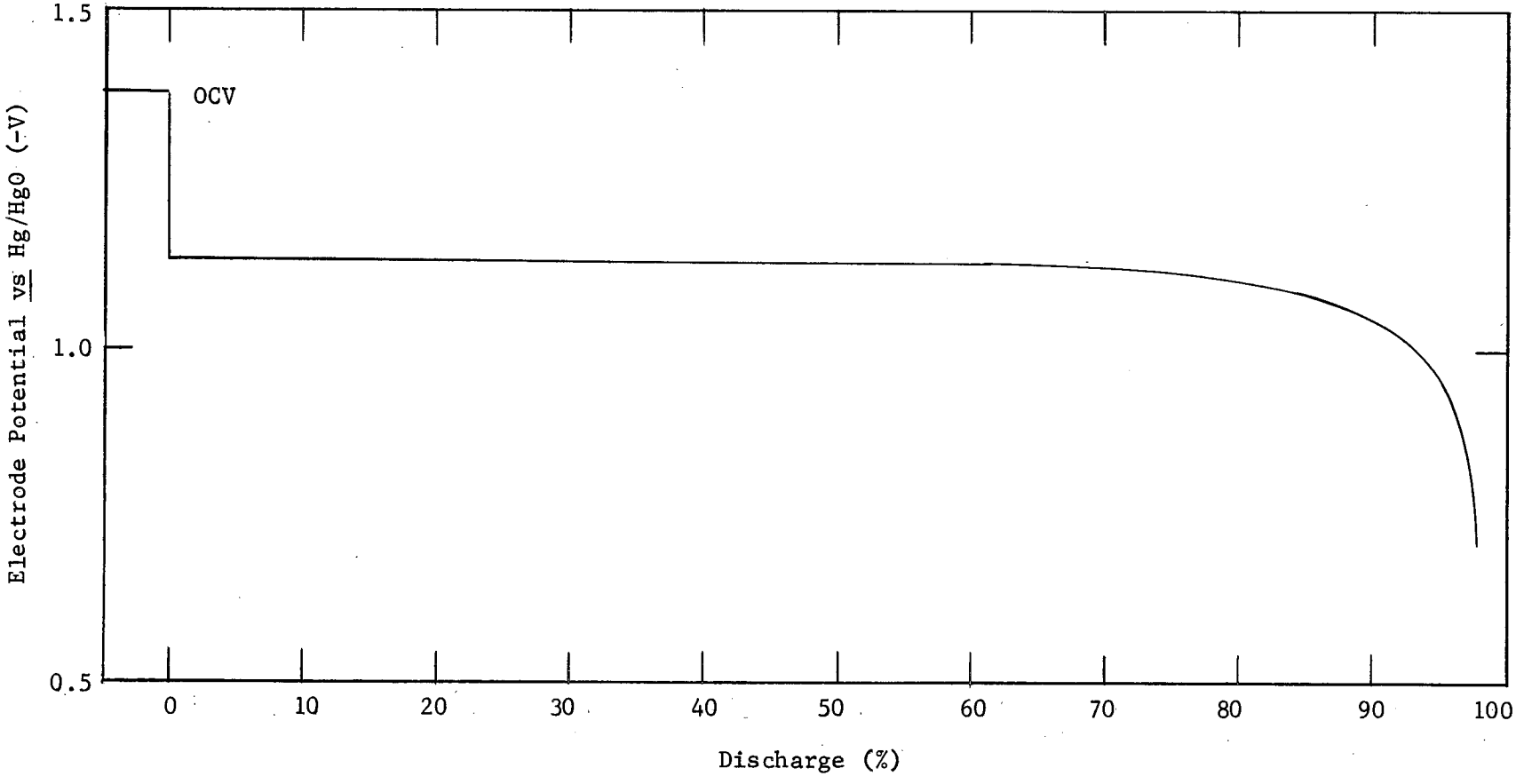

Figure 7. Discharge of Zn(Hg) Electrode in 10 VF KOH at 219 mA/cm^2

The aqueous systems proved most satisfactory for high-discharge anodes. Typical discharge curves are shown in Figure 8. All discharge curves were similar in form at all discharge rates with a fairly flat curve being obtained over most of the discharge even though there was as much as a 15-fold difference in current-density. The break at about 20% discharge was typical at the 1,200 mA/cm^2 rate, but disappeared at higher rates, probably because it was "smeared out" by the rapid reaction.

The use of amalgam hanging-drops allowed maximum current-densities of greater than 8 A/cm^2. The effect of both high-rate charge and high-rate discharge on charge recovery was measured and is shown in Tables 1 - 4 for K(Hg) systems where electrolyte concentrations are 10 VF and saturated.

There appears to be a decrease in recovery with increasing discharge rate in the range between 300 mA/cm^2 and 4.0 A/cm^2. Above this range, recovery seems relatively independent of the rate.

The initial charge seems to have a definite effect on recovery in both saturated and 10 VF systems. In the saturated system, the recovery was 99% with an initial charge of 4.5×10^{-5} A-hr while it was only 90% with an initial charge of 8.3×10^{-5} A-hr. Similarly, recovery in the 10 VF KOH system was 99% at 4.5×10^{-5} A-hr and 82% at 8.8×10^{-5} A-hr. The higher charge brings the amalgam closer to saturation and some gassing may occur during charge. However, recovery was good at low discharge rates (<1 A/cm^2) and high initial charge. Transport to and from the electrode surface should be relatively slow compared with the reaction rates at high current-densities so that the electrode may become somewhat less efficient under these conditions.

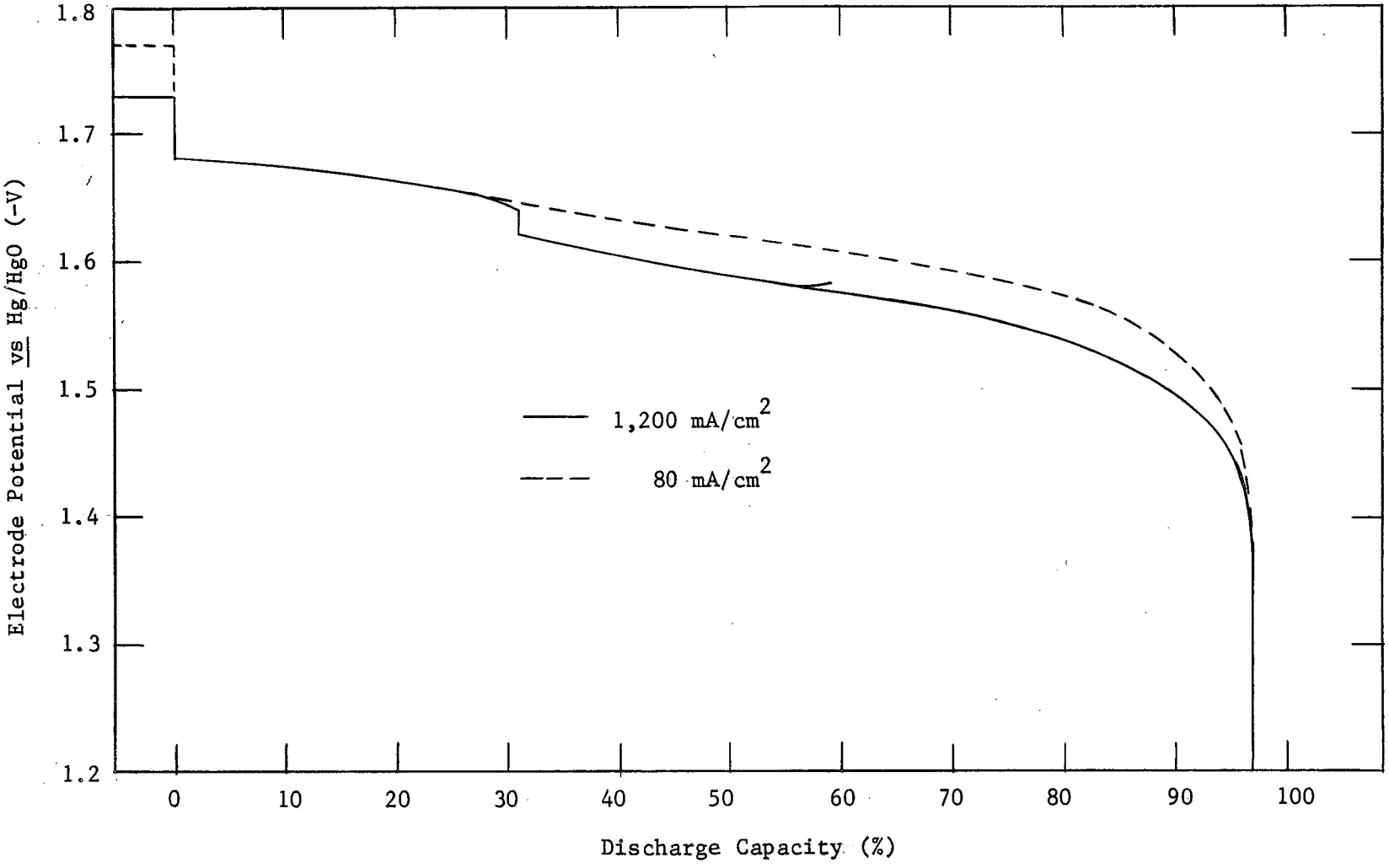

Figure 8. Discharge of K(Hg) Electrode

Table 1

Effect of Discharge Rate on Electrode Capacity

Electrolyte solution is saturated KOH. Electrode A = 0.0327 cm^2 and is charged at 26 mA/cm^2. Precision of measurements is given at the 95% confidence level. No precision is indicated if less then three measurements were made.

No. of Runs	Total Charge (A-hr x 10^5)	Discharge Current-Density (mA/cm^2)	Charge Recovery (%)
2	8.3	134	100
2	8.3	269	100
2	8.3	538	97.5
3	8.7	1344	91.7 ± 12.7
2	8.3	2688	90
3	4.5	2688	99.0 ± 2.5
2	9.0	4037	78.5
3	8.8	5376	77.3 ± 7.6
1	8.7	6720	74
3	8.4	7527	81.0 ± 4.3
8	8.6	8065	81.4 ± 2.6

Table 2

Effect of Discharge Rate on Electrode Capacity

Electrolyte solution is 10 VF KOH. Electrode A = 0.0368 cm^2 and is charged at 26 mA/cm^2. Precision of measurements is given at the 95% confidence level.

No. of Runs	Total Charge (A-hr x 10^5)	Discharge Current-Density (mA/cm^2)	Charge Recovery (%)
4	8.8	2717	87.8 ± 9.3
2	4.6	2717	99
4	8.9	4076	75.7 ± 2.4
6	8.6	5435	75.8 ± 8.2
8	8.1	6793	79.2 ± 4.4
4	8.3	7473	72.8 ± 17.0
12	7.6	8152	77.6 ± 3.9

Table 3

Effect of Charge Rate on Electrode Capacity

Electrolyte solution is saturated KOH. Electrode A = 0.0327 cm^2 and is discharged at 134 mA/cm^2. Precision of measurements is given at the 95% confidence level.

No. of Runs	Total Charge (A-hr x 10^5)	Charge Current-Density (mA/cm^2)	Charge Recovery (%)
5	3.6	2688	99.4 ± 1.1
3	1.5	5376	95.7 ± 9.4
4	1.3	6720	97.5 ± 4.0
9	1.3	8064	75.8 ± 3.5
9	0.78	8064	89.0 ± 4.3

Table 4

Effect of Charge Rate on Electrode Capacity

Electrolyte solution is 10 VF KOH. Electrode A = 0.0368 cm^2 and is discharged at 135 mA/cm^2.

No. of Runs	Total Charge (A-hr x 10^5)	Charge Current-Density (mA/cm^2)	Charge Recovery (%)
2	4.6	2717	99
2	2.3	5435	94
2	1.3	8152	84
2	0.98	8152	96

Charge rates have less effect on recovery than do discharge rates. Recoveries of about 90% were obtained in both saturated and 10 VF systems at rates of about 8.1 A/cm^2. Amount of charge affects recovery in much the same way as at high discharge rates. The mechanism is not known but must be different from that in the discharge case because the discharge rate (134 mA/cm^2) is relatively low here.

A preliminary attempt was made to measure the OCV of K(Hg) electrodes at different total charges (amalgam concentrations). The results are shown in Table 5. The results are roughly what one would expect except that the increase with charge above a total of 3 mA-hr/g Hg is much lower than one would predict. Although some self-discharge is expected, it does not occur rapidly enough to cause an apparent leveling of the OCV at the higher charges.

The several materials chosen as active substances for amalgam cathodes were selected on the basis of their standard potentials[8] and their tendency to dissolve in the electrolyte chosen. Most were known to dissolve fairly readily in alkaline solution through the formation of soluble hydroxy-complexes.

Gold chloride, $AuCl_3$, should readily reduce to the metal which is easily amalgamated. However, $AuCl_3$ is not very soluble in 10 VF KOH and it oxidizes mercury quite readily.

Stannous oxide is fairly soluble in alkaline solution, but disproportionates rapidly to form the metal and the insoluble SnO_2[9].

Gold and silver ammines were discarded since they are known to form dangerously explosive "fulminates". However, copper apparently forms no such substance and is very soluble in concentrated ammonia. A cell was constructed using a mercury pool in a $Cu(NH_3)_4^{2+}$ - NH_3 solution; this was discharged through a power supply. Fairly high current-densities were obtained (>1 A/cm^2), but the cell resistance was extremely high, possibly

Table 5

Potassium-amalgam Open-circuit Potentials

Capacity (A-hr/g Hg)	OCV vs Hg/HgO* (V)
0.001	1.74626
	1.74341
0.002	1.77806
	1.77514
0.003	1.80312
	1.80224
	1.80326
0.004	1.80601
0.005	1.80612
0.006	1.80640

*Potential of Hg/HgO reference is +0.098V.

because ammonia is only slightly dissociated. The concentration of the $Cu(NH_3)_4^{2+}$ was insufficient to provide a highly conducting system.

The $Zn(Hg)/Zn(OH)_4^{2-}$, KOH cathode gives apparent current-densities in excess of 5 A/cm^2 when operated through a power supply, but only about 200 mA/cm^2 when used in a battery with a K(Hg)/KOH anode. The two-step reduction of Zn(II) described earlier accounts for this behavior. Thus, the electrode is of little use as a cathode.

Selenium and tellurium amalgams have some promise as cathodes. Crude cells of the type shown in Figure 9, in which a K(Hg)/KOH anode was used, were constructed. On "short-circuit", the selenium cathode showed a current-density of about 200 mA/cm^2--not remarkable, but quite good for this configuration. The tellurium cathode, while showing only 70 mA/cm^2, had an amazingly constant voltage until the end of discharge. Thus, these cathodes may prove useful with further development.

A K(Hg)/KOH - Tl(Hg)/KOH cell, having the configuration of Figure 9, was operated with some success. Where a cellophane separator was used, the cell produced a maximum current-density of about 1.1 A/cm^2 and, in fact, maintained a value in excess of 1.0 A/cm^2 for three minutes. A similar cell using sausage casing produced a maximum of about 0.78 A/cm^2 and a steady value of 0.63 A/cm^2 for 1.3 minutes.

The thallium-amalgam cathode has serious disadvantages. It is not rapidly recharged, the maximum satisfactory current-density being about 3 mA/cm^2. The TlOH is not soluble in excess base and tends to form crystals on the separator between the anode and cathode compartments. Ultimately, this would increase cell resistance, decrease availability of Tl(I) in the cathode compartment, and would probably lead to separator failure. However, these problems should not be insurmountable and the electrode does show promise otherwise.

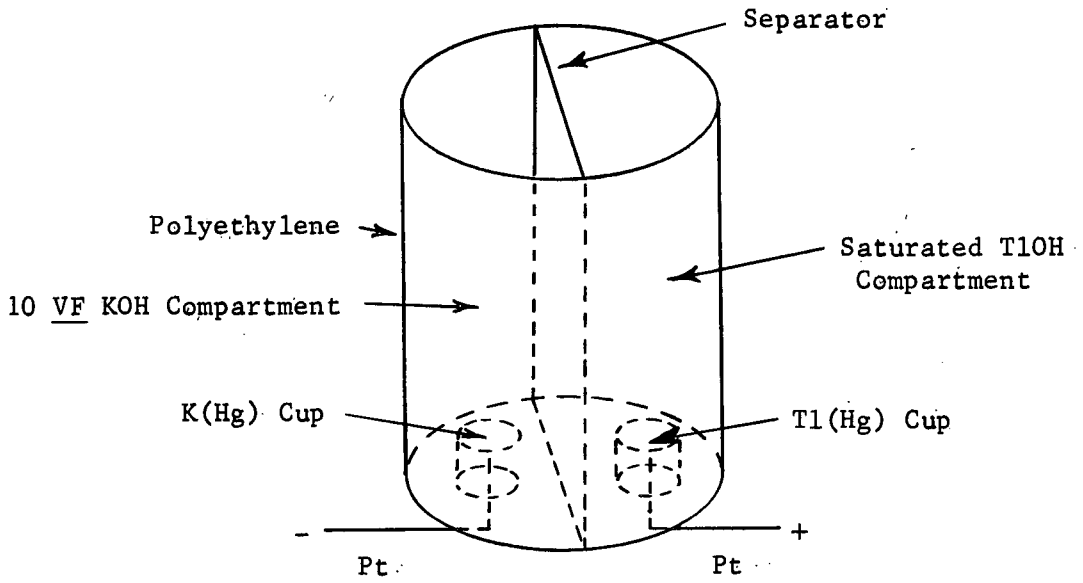

Figure 9. K(Hg) - Tl(Hg) Cell Configuration

The stand-life of the electrodes used in any battery system is important since it indicates how long the battery can rest without recharge and, indirectly, indicates the probability of pressure build-up in sealed batteries. As might be expected, rate of self-discharge is dependent on the electrolyte concentration. This is represented by the equation:

$$M + xH_2O \rightarrow M(OH)_x + \frac{x}{2}H_2 \qquad (1)$$

Thus, as the electrolyte concentration is increased, the water activity is decreased so that the tendency for the reaction to proceed is also decreased. If a hydroxy-complex is formed with the metal, this effect may be somewhat modified by the equilibrium:

$$M(OH)_x + yOH^- \rightleftharpoons M(OH)^{y-}_{(x+y)} \qquad (2)$$

However, reaction (1) is probably irreversible and its rate should not be seriously affected by the equilibrium. These conclusions are supported by the results shown in Tables 6 - 8. Table 6 indicates quite graphically the effect of electrolyte concentration on stand-life. Although the data are scattered, the trend is as expected. It should be noted that the Zn(Hg) electrode seems quite stable in 10 VF KOH with virtually no loss over about one month.

Table 7 shows the stand-life of the potassium-amalgam electrode to be limited in 10 VF KOH. In all cases, recovery was less than 50% after 15 days. A battery containing this electrode would probably have to be kept on trickle-charge and, if sealed, would tend to build up considerable pressure.

Table 6

Stand-Life of Zn(Hg) Electrodes

Discharge Rate = 16.7 mA/cm^2

KOH Concentration (VF)	Total Charge (A-hr)	Charge Rate, (mA/cm^2)	Stand Time (hours)	Discharge Capacity (%)
1	0.125	2.0	169	79
			363	59
			510	37
			752	60
2	0.0725	1.7	100	84
			317	80
			653	85
10	0.1015	2.3	27	99
			265	100
			672	100

Table 7

Stand-Life of K(Hg) Electrodes in 10 VF KOH

OCV is the measured value at the end of the stand time and before discharge. Discharge rate = 50 mA. Each value represents an individual electrode.

Charge (mA-hr)	Stand Time (hours)	OCV vs Hg/HgO (V)	Recovery (%)
68	0.17	-1.68	81
	35	-1.70	84
	157	-1.67	68
	302	-1.67	43
	455	-1.59	0
101	0.08	-1.73	96
	311	-1.67	25
	312	-1.50	0
	312	-1.60	2
105	1.15	-1.69	54
	1348	-1.54	0
	1348	-1.69	47
	1561	-1.66	15
105	0.5	-1.67	21
	1370	-1.00	0
	1371	-1.64	7
	1371	-1.67	16

Table 8 shows a similar type of electrode in a saturated KOH solution. In this case, self-discharge was considerably decreased with an electrode showing 85% recovery after a stand of 0.7 year. From this standpoint, the saturated electrolyte has a definite advantage over any others. However, this electrode has tended to be noisy on high-rate discharge and so has not been investigated further.

Table 8

Stand-life of K(Hg) Electrodes in Saturated KOH

Charge (mA-hr)	Stand Time (hours)	OCV vs Hg/HgO	Recovery (%)
105	768	-1.68	98
	1802	-1.64	94
	6100		85

None of the stand-life electrodes were fully charged. Other experiments have indicated higher relative recovery with higher total charge. Thus, the percentages, in all cases, might be higher. However, there is also some indication of higher absolute self-discharge rates at higher charge; this could complicate fabrication of a sealed system.

Considerable work has been expended in attempts to fabricate working cells and batteries. In most cases, these have utilized K(Hg) anodes and Ag/AgO cathodes and the rectangular configuration of Figure 3. A few have used Na(Hg) anodes and others have used Ni/NiOOH cathodes.

All cells and batteries were discharged into resistances of 15 ohms or less and most into a "short-circuit" at some time. Typical discharge

curves are shown in Figures 10 - 12. Figure 10 shows a typical "short-circuit" discharge. The voltage dropped to quite a low value and remained fairly constant throughout the discharge. Obviously, a true short-circuit is not attained since, by definition, no voltage-drop can occur across it.

The discharge curve for a Na(Hg)-10 VF NaOH-Ag/AgO cell into a 15-ohm load is shown in Figure 11. This is a typical curve whether the anode is Na(Hg) or K(Hg). The drop early in the discharge was probably caused by the complete reduction of AgO to Ag_2O. Thereafter, the curve was quite flat until discharge was complete.

Figure 12 shows the behavior of a cell in which a saturated NaOH solution was used. Here, the last portion of the curve shows poor characteristics which might be attributed to formation of solid NaOH on the mercury-separator interface.

These curves are typical of all of the batteries built with the rectangular configuration. In many cases, there was noise at high rates which, although not shown in the figures here, would appear as very sharp spikes on a recorder trace. Details differ from cell to cell, depending on fabrication and components used, but the behavioral form remained the same throughout.

A number of simple cells was built, all using the Figure 3 configuration. These consisted of one cathode and one anode having nominal surface areas (one side) of 10 cm^2. They were all discharged into "short-circuits".

Table 9 shows results typical of a K(Hg)-10 VF KOH-Ag/AgO cell using a cellophane separator. It can be seen that virtually all of the charge was recovered in these discharges. Discharge current-densities approached 1 A/cm^2 which was thought to be very good for a silver electrode when these experiments were run. Currents remained quite high for relatively long periods. Where cellophane was used, the discharge was noisy during the

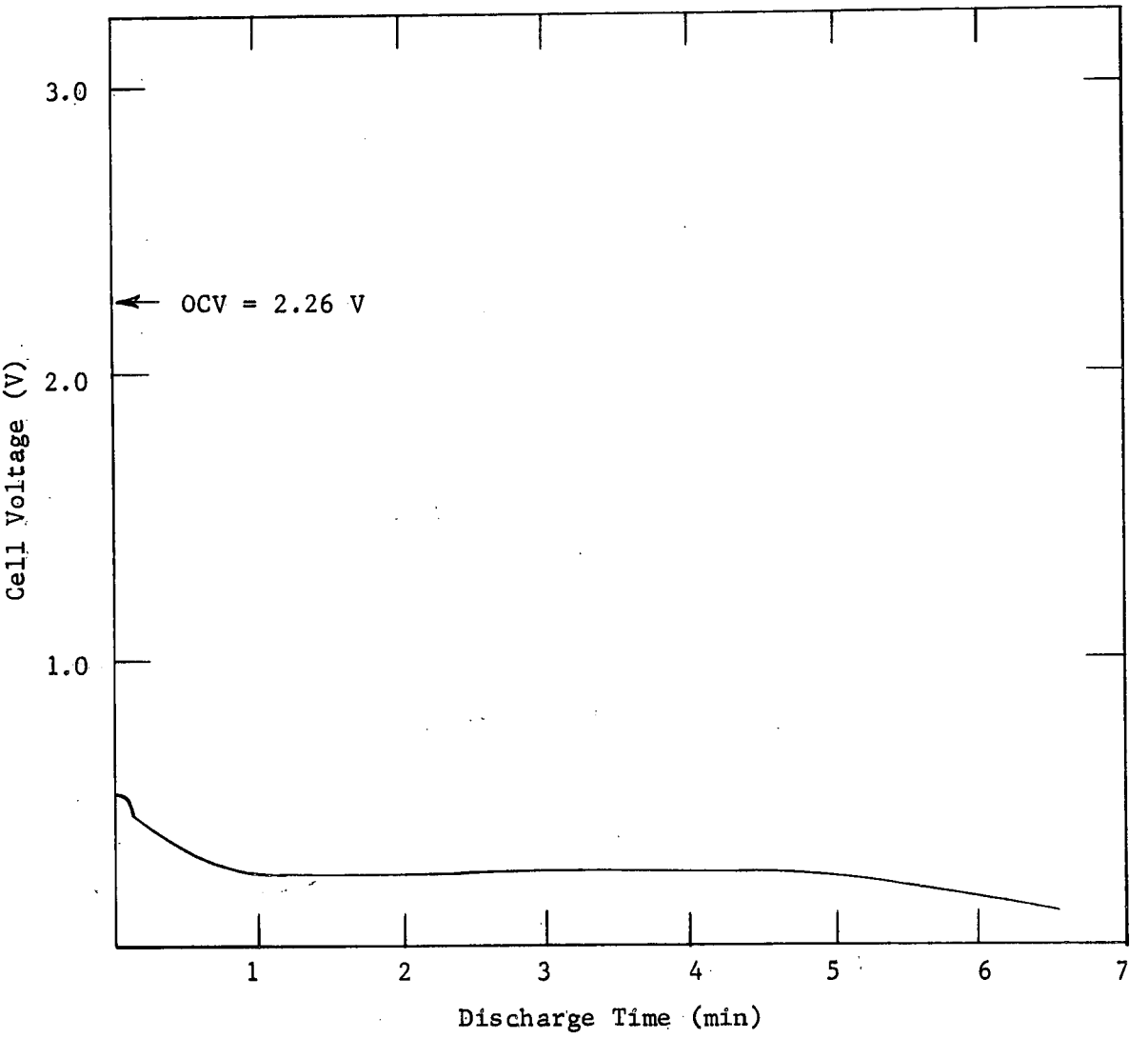

Figure 10. Short-circuit Discharge of K(Hg) - Ag/AgO Cell

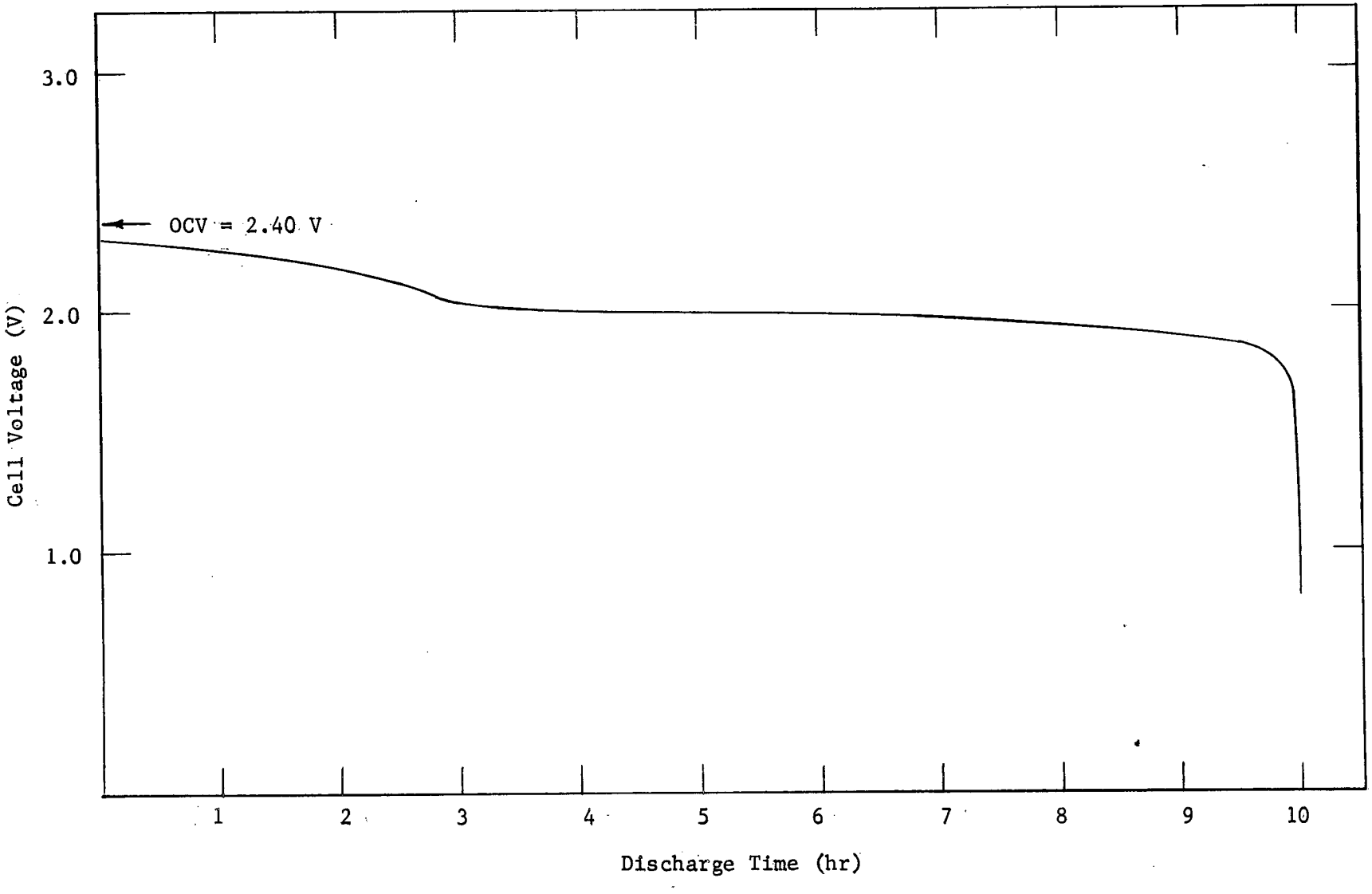

Figure 11. Discharge of Na(Hg) - 10 VF NaOH - Ag/AgO Cell into 15 ohms

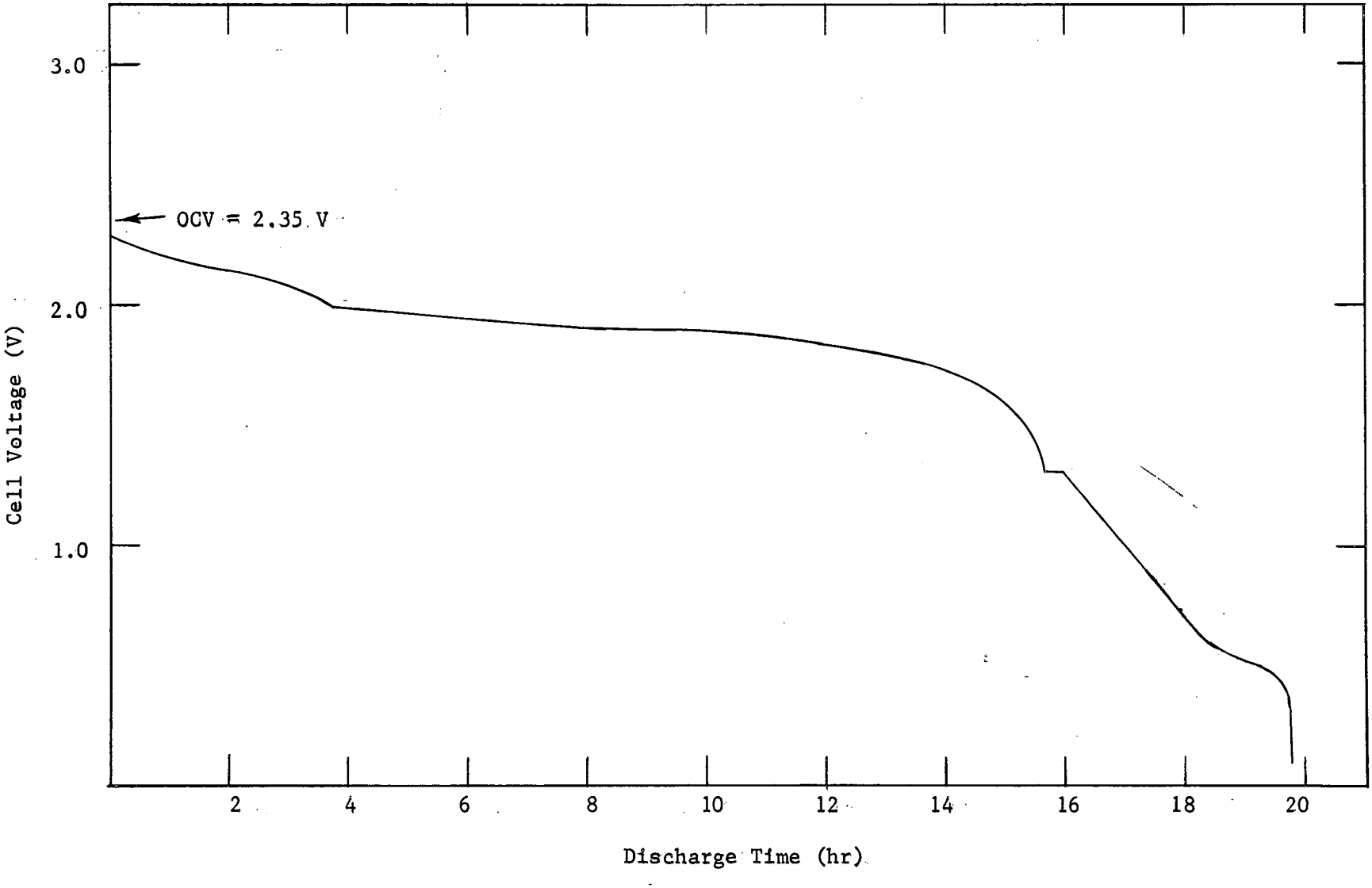

Figure 12. Discharge of Na(Hg) - 15.3 VF NaOH - Ag/AgO Cell into 15 ohms

Table 9

Operation of K(Hg) - Ag/AgO Cell

Nominal cathode A = 10 cm^2. One anode and one cathode. Separator: one layer of cellophane cemented on each side of ceramic spacer. All discharges "short-circuit".

	Charge				Discharge				
Cycle	I(mA)	Time(hours)	A-hr	OCV(V)	Max. I(A)	Final I(A)	A-hr	OCV(V)	Remarks
1				2.26	8.0				Noisy first 30 sec. Steady between 2.5 & 2.2 A for 3 min.
2	50		0.15	2.23	9.6	2.0	0.15	1.80	Noisy between 5 & 7A
3	50	0.75							
	25	3.3							
	5	12.96	0.18	2.23	8.0		0.18	1.80	
4	50	2.0							
	25	3.0	0.175	2.23	8.8	2.0	0.18		Steady for 1 min. at 4.4 A
5	50	2.0							
	25	3.5	0.19	2.23	8.2	2.0	0.19	1.72	
6	10	11.25							
	25	3.7	0.20	2.24	9.0	2.0	0.20		Noisy between 6 & 7A. Steady 4.9 A for 30 sec.
7	50	3.3	0.165	2.24	8.5	0.7	0.16		Noisy first 30 sec.

first half-minute. The noise was not a "hash" but appeared as discrete spikes of one or two volts several seconds apart. Although none have been observed directly, it seems that gas bubbles might have been formed periodically which temporarily produced high cell-resistance. In any case, the phenomenon seemed to occur only when cellophane separators were used.

Table 10 shows the results for a similar cell using a sausage-casing separator. The cell failed after only three cycles. It is notable that both the maximum current and the charge recovery increased with the number of cycles leading to the conclusion that, had it survived, this cell might have performed better than the previous one after a break-in period. Furthermore, no noise was observed at any time during the discharges. Nevertheless, low cycle-life led to the abandonment of sausage casing in most of the later systems.

Table 11 shows the results of a cell using MBS-1 as the separator. Maximum currents were definitely lower and charge recovery was poor which suggests that the separator resistance was fairly high compared with that of cellophane. MBS-2 showed similar behavior. The discharges were not noisy.

A Na(Hg)-10 VF NaOH-Ni/NiOOH cell was discharged with results shown in Table 12. Both current maxima and charge recovery were inferior to those observed for the K(Hg)-10 VF KOH-Ag/AgO cells. The first discharge was noisy but subsequent discharges were remarkably smooth.

The lack of noise in this last case is interesting since the cell employed a cellophane separator. This would suggest that noise is brought about by an interaction between AgO and cellophane. However, current maxima were considerably higher in the silver systems; had they been as high in the nickel cell, similar noise might have been observed. The phenomenon deserves further investigation.

Table 10

Operation of K(Hg) - Ag/AgO Cell

Nominal cathode A = 10 cm^2. One anode and one cathode. Separator: one layer of sausage casing cemented to spacer. All discharges "short-circuit".

	Charge				Discharge				
Cycle	I(mA)	Time(hour)	A-hr	OCV(V)	Max. I(A)	Final I(A)	A-hr	OCV(V)	Remarks
1	50			2.24	6.0	0.9		1.95	
2	50	1.67							
	25	1.67	0.125	2.27	8.0	2.0	0.095		
3	50	1.4							
	25	3.1	0.148	2.27	9.2	2.0	0.140		Steady at 2.2 A for 1.5 min.

Table 11

Operation of K(Hg) - Ag/AgO Cell

Nominal cathode A = 10 cm^2. One anode and one cathode. Separator: one layer of MBS-1 cemented to spacer. All discharges "short-circuit".

	Charge				Discharge				
Cycle	I(mA)	Time(hour)	A-hr	OCV(V)	Max. I(A)	Final I(A)	A-hr	OCV(V)	Remarks
1	25	7.0	0.175	2.27	4.0	1.0	0.094	2.08	Steady at 1.1 A for 1.5 min.
2	5	10.7	0.053	2.22	4.0	1.0	0.040	2.00	Steady at 1.2 A for 1 min.

Table 12

Operation of Na(Hg) - Ni/NiOOH Cell

Nominal cathode A = 9.6 cm^2. One cathode and one anode. Separator: one layer of cellophane cemented to spacer. All discharges "short-circuit".

	Charge				Discharge				
Cycle	I(mA)	Time(hour)	A-hr	OCV(V)	Max. I(A)	Final I(A)	A-hr	OCV(V)	Remarks
1		Pre-charge			6.0				Very noisy
2	10	13.3	0.133	2.30	6.0	1.0	0.074	2.10	Ni gasses. OCV = 2.22 V after 25 hr OC. Discharge very smooth. E = 0.2 V at 1.2 A
3	10	22.5	0.225	2.35	5.8	1.0	0.152	1.80	Very smooth discharge. Current 1.2 A @ 2 min. and held steady for 2.5 min.

Several K(Hg)-10 VF KOH-Ni/NiOOH cells have been constructed employing more than one of each kind of electrode. The behavior of one such cell is shown in Table 13. Maximum currents on "short-circuit" generally exceeded 30 A and increased with cycle number.

The behavior of a second K(Hg)-10 VF KOH-Ni/NiOOH cell employing larger electrodes is shown in Table 14. The total plate area was about 4.5 times that of the former cell while the maximum current was somewhat less than proportional. The differences are probably not significant. The larger cell used sausage-casing for the separator while the smaller one used cellophane.

Table 15 shows the behavior of a K(Hg)-10 VF KOH-Ni/NiOOH cell employing six of each of the smaller electrodes with cellophane separators. Behavior was generally good, but elements shorted out readily.

In general, cells employing nickel cathodes seemed to give higher "short-circuit" currents than comparable cells using silver. However, no facilities were available for fabricating nickel electrodes and those obtained from commercial sources proved difficult to adapt. When the nickel electrode is cut, it tends to slough off active material and it does not hold up well during cycling. However, it does seem that the K(Hg)-Ni/NiOOH and Na(Hg)-Ni/NiOOH systems should be investigated further.

Several K(Hg)-10 VF KOH-Ag/AgO batteries were built in the Figure 3 configuration. Table 16 shows the behavior of a 3-cell battery in which each cell contained three silver and three amalgam electrodes. Discharge behavior was very good but cycle-life was poor. The "short-circuit" current was remarkably high with peak currents over 200 A. Note that peak current transients persisted for 0.2-0.5 second. It should be noted, also, that the "short-circuit" discharges were with one cell shorted, thus decreasing the battery voltage without decreasing its resistance.

Table 13

Operation of K(Hg) - Ni/NiOOH Cell

Nominal cathode A = 11 cm^2. Two cathodes and one anode. Separator: one layer of cellophane cemented to spacer. Charged at constant voltage. All discharges "short-circuit".

	Charge		Discharge							
Cycle	A-hr	OCV(V)	Max. I(A)	E(V)	Final I(A)	E(V)	Duration	A-hr	OCV(V)	Remarks
1		2.24	30	0.35	18					
2	0.39	2.24	40		8			0.33	1.97	Noisy discharge
3	0.36	2.24	57		8			0.27		Little noise

Table 14

Operation of K(Hg) - Ni/NiOOH Cell

Nominal cathode A = 49.6 cm^2. Two cathodes and one anode. Separator: one layer of sausage-casing cemented to spacer. All discharges "short-circuit". 10.2 VF KOH.

		Discharge				
Cycle	OCV(V)	Max. I(A)	E(V)	Final I(A)	A-hr	Duration (min)
1		142	0.033	- 19	1.33	3
2	2.20	164	0.046	21	1.28	2.3
3	2.21	154	0.038	17	0.87	1.7

Table 15

Operation of K(Hg) - Ni/NiOOH Cell

Nominal cathode A = 11 cm^2. Six cathodes and six anodes. Separator: one layer of cellophane cemented to spacer. Charged at constant voltage. 10 VF KOH.

	Charge		Discharge							
Cycle	A-hr	OCV(V)	Load(ohms)	Max. I(A)	E(V)	Final I(A)	E(V)	A-hr	Duration	Remarks
1		2.21	15	0.147	2.21	0.121	1.81		8 hr	
						0.081	1.21		12 hr	Cell became noisy
								1.46	13 hr	Shorted
2	1.50	2.19	1	2.03	2.03		1.63		0.25 hr	
							0.60		0.75	Noise
							0.55	0.75	1.5	Cell shorted out

Table 16

Operation of K(Hg) - Ag/AgO Battery

Outside dimensions: 3.7 cm x 4.5 cm x 8.5 cm. Nominal cathode area = 11 cm^2. Three cathodes and three anodes per cell; three cells. Separator: one layer of cellophane cemented to spacer. 10 VF KOH. Charge at constant voltage.

		Discharge						
Cycle	OCV(V)	Load(ohms)	Max. I(A)	E(V)	Final I(A)	E(V)	Duration(min)	Remarks
1	6.91	1.45	3.9	5.65		5.3	1	
						5.0	8.75	
2	6.95	1.05	5.24	5.5		5.0	1.8	
						4.5	3.8	
						3.7	9.5	
					3.4	3.5	10.5	
3	4.58	short	232	0.058	50		0.2	One cell out
					20		1	
4	4.58	short	216	0.054	50		0.2	
					10		1.0	
					5		1.8	

Table 17 shows the behavior of a similar 4-cell battery. Again, behavior was quite good and cycle-life was slightly better. "Short-circuit" maximum current was considerably lower indicating a higher resistance in the failed cell.

Table 18 shows the behavior of a 5-cell battery. Behavior, except for cycle-life, was quite good. The maximum "short-circuit" current was remarkable while a current above 40 A for 21 seconds is commendable. Unfortunately, this treatment caused one cell to be destroyed. Even more remarkable was the single-cell current considering that this followed without recharge of the battery. Finally, the battery discharge, without prior recharge, into the 1-ohm resistor was higher than expected.

Considering the <u>total</u> nominal area of the silver electrode, i.e., both sides of each plate, the maximum current-density (Cell #3) was 2.9 A/cm^2. This is considerably higher than any previously observed for the silver electrode. Possibly the cell resistance was unusually low. However, one is left with the impression that more investigation of the silver electrode at high discharge-rates would be in order.

Finally, a 6-cell battery was constructed. This battery had an OCV of 13.6 V and delivered 10.8 V at 10.8 A into a 1-ohm load. The voltage decreased linearly to a final value of 6.0 V in about 5 minutes. A "short-circuit" discharge of one of the cells delivered a peak current of 240 A: the current remained greater than 50 A for 30 seconds. Cycle-life was poor.

The favorable high-discharge behavior of the systems described above suggested that high currents might be obtained from small, button-type cells. One constructed as described and diagrammed in Figure 4 gave the discharge behavior shown in Figure 13. Discharge characteristics are seen to be quite excellent. The configuration of Figure 4 is hardly optimum because many complications are produced in a horizontal array since gas pockets tend to

Table 17

Operation of K(Hg) - Ag/AgO Battery

Outside dimensions: 3.7 cm x 4.5 cm x 11.5 cm. Nominal cathode A = 11 cm^2. Three cathodes and three anodes per cell: four cells. Separator: one layer of cellophane and one layer of polypropylene. 10 VF KOH. Charged at constant voltage.

	Charge		Discharge								
Cycle	A-hr	OCV(V)	Load(ohms)	Max. I(A)	E(V)	Final I(A)	E(V)	Duration(min)		A-hr	OCV(V)
1	Pre-charge	9.18	1.05	6.92	7.26		6.50	2.0			
							6.00	2.5			
							6.00	4.0			
						4.4	4.60	4.5		0.508	8.2
2	0.44	9.21	1.05	6.8	7.19		6.25	2.4			
							5.5	3.4			
							5.4	4.9			
						4.3	4.5	5.6		0.53	8.2
3	0.726	9.21	15.0	0.581	8.72		7.0	78			
							5.5	81			
						0.333	5.0	98		0.728	8.07
4		6.89	short	90		25		One cell out			

Table 18

Operation of K(Hg) - Ag/AgO Battery

Nominal cathode A = 11 cm^2. Three cathodes and three anodes per cell: five cells. Separator: one layer of cellophane and one layer of polypropylene. 10 VF KOH. Charges at constant voltage.

	Charge		Discharge								
Cycle	A-hr	OCV(V)	Load(ohms)	Max. I(A)	E(V)	Final I(A)	E(V)	Duration	A-hr	OCV(V)	Remarks
1	Precharge	11.7	1.03	8.96	9.23	5.9	6.11	7.7 min	1.01		Linear with time
2	0.792	11.7	15.0	0.733	11.0	0.593	8.9	81 min	0.88		Linear with time
3	0.800	9.21	short	320	0.080	40		21 sec		6.1	One cell shorted Peak I for 0.5 sec
		Short each cell		100							#1 cell
				200							#2 cell
				150							#3 cell
			1.03	5.5	5.70		3.10		0.5		Smooth decrease

form at the separator. Furthermore, the distance between plates is excessive.

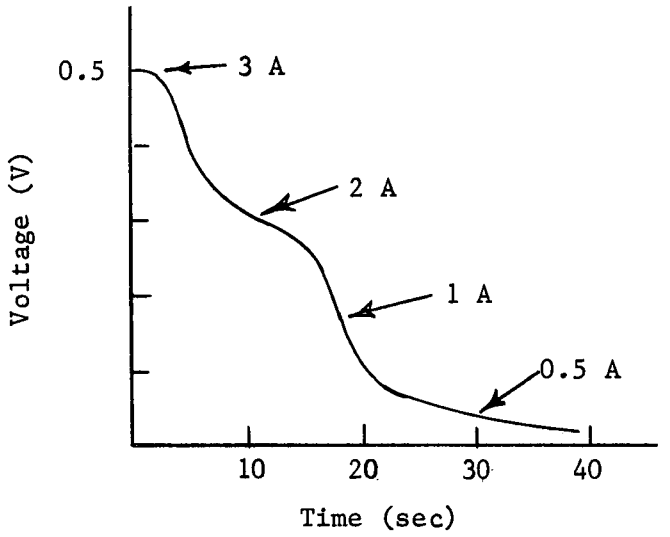

Figure 13. Discharge of Button Cell

No doubt better engineering could result in even higher discharge rates in a secondary cell of reasonable cycle-life but having dimensions similar to those of the button cell described here. Again, it should be noted that the nominal current-density for the cathode was surprisingly high.

Suggested Work

The amalgam batteries show great promise as special-purpose devices which can deliver high currents from small packages. Further work on an engineering scale is needed to develop them into useful primary and/or secondary batteries. Containment of the amalgam, suppression of gassing, and development of adequate separators are some of the problems in need of solution.

No attempt has been made to study the temperature dependence of the amalgam behavior. Mercury freezes at -40°, but amalgamation could depress

the freezing point considerably and thus make the amalgam useful at lower temperatures. No information is available on these points.

The work with Ag/AgO cathodes has indicated further areas of research in the study of high discharge-rates. The remarkably high nominal current-densities observed in a number of cases lead to the suspicion that these electrodes have not been utilized to their maximum capabilities.

Further investigation of amalgam cathodes is probably worthwhile. The Tl/TlOH electrode seems particularly promising since fairly high current-densities were achieved in a very inefficient cell. Other possible systems should be sought, also.

B. DEPOSITION OF SILVER ON ZINC ELECTRODES

Introduction

The rate of self-discharge by direct interaction of Ag(I) with zinc will depend on the rate of the chemical reaction, the rate of solution of the AgO electrode in the KOH solution, and the rate of transport of the silver species through the separator and the electrolyte solution. All evidence suggests that the rate of chemical reaction is very rapid; the assumption is made, therefore, that this mechanism need not be considered. Diffusion through the separator is being studied by other workers and will not be a part of this work.

The solubility of AgO and Ag_2O in KOH solutions has been measured by several workers[10,11,12]. Equilibrium concentrations of Ag(I) ranging from 2×10^{-4} VF to 5×10^{-4} VF have been reported. Amlie and Ruetschi[12] report that no Ag(II) exists in KOH solutions in equilibrium with AgO, hence designation of solubilities of AgO as well as Ag_2O in terms of Ag(I) concentration seems justified. Solubilities measured in this laboratory by a polarigraphic technique[13] gave values of about 4×10^{-4} VF[1] in 10 VF KOH. Still,

another independent determination seemed advisable in view of the scattering of data previously reported. A tracer method was chosen.

While reaction of Ag(I) with zinc will cause self-discharge of the zinc electrode, this can be nullified by keeping the cell under an appropriate trickle-charge or by recharge. However, the silver deposited will remain unchanged and may affect the behavior of the zinc electrode. Therefore, a series of chronopotentiometric experiments was initiated to measure these effects.

Although the chronopotentiometric method seemed to offer a relatively fast method for determining the diffusion coefficient of the silver species, the chronopotentiograms were too complicated to allow ready interpretation. This complexity may be caused in part by the diffusion of several species at different rates. Several such species have been proposed by Biedermann and Sillen[11]. Since the requirements here are for a composite diffusion rate, the capillary method of Anderson and Saddington[14] was finally selected.

Experimental

Solubility A tracer method was used to determine the Ag(I) concentration in the electrolyte solutions. The stock solution was 0.0252 VF in Ag(I) and contained an appropriate amount of ^{110m}Ag. Measurements were made with a Nuclear-Chicago Model 703 liquid-scintillation counter system.

Unless otherwise specified, all chemicals were J. T. Baker Reagent Grade. 2,5-diphenyloxazole (PPO) and dimethyl-2,2-p-phenylenebis(5-phenyloxazole)(dimethyl-POPOP) were obtained from the Packard Instrument Co. AgO was obtained from Ames Chemical Works.

The composition of the scintillator cocktail was 7 g/l of PPO, 0.3 g/l of dimethyl-POPOP, and 100 g/l of naphthalene in p-dioxane stabilized with sodium diethyl-dithiocarbamate.

Rate of deposition

The temperature was controlled at 25° ± 0.1° in all experiments. One milliliter of silver stock was pipetted into about 50 ml of 10 VF KOH in a polyethylene bottle. A piece of sheet zinc was hung in the solution on a glass hook, the bottle was capped, and the system stirred. Periodically a portion of the solution was withdrawn and centrifuged, 50λ of the supernatant was pipetted into 15 ml of scintillation cocktail, and the remainder was returned to the reaction bottle.

Effect of silver deposit on electrode behavior

Chronopotentiometric transition times were measured with a Labline timer accurate to 0.1 second. Constant current was supplied by a Model C629CMK Electronics Measurements power supply. Potential-time traces were made with a Dohrmann Model RSC1100 multirange recorder. The cell consisted of a sheet-zinc disc cut to fit the top of a 20-ml polyethylene vial. The screw threads were dipped into hot paraffin and the disc was mounted and held in place by screwing on the vial cap. Electrical connection was made through the cap. The bottom of the vial was cut out to allow insertion of solution, auxiliary electrode, and salt bridge. The auxiliary electrode was a small platinum sheet placed inside a tube having a fritted-glass end. The reference electrode was Hg/HgO in 10 VF KOH.

Diffusion of Ag(I)

The diffusion cell was constructed from capillary tubing of about 1 mm I.D. by carefully sealing the tubing in a flame and flattening the end. The length of the cavity was measured by inserting a straight piece of wire, cutting, and carefully grinding it flush with the open end of the cell. The wire was removed and its length measured with a micrometer. The capillary was mounted on a plastic disc which was attached to a glass support rod.

The whole was mounted in a rubber stopper which served as the top of the main cell chamber.

The main cell chamber contained 40 ml of 9.94 VF KOH saturated with Ag_2O. The capillary cell was filled with the same solution which also contained added ^{110m}Ag tracer. The capillary cell was mounted in the main solution with the open end above the surface and the complete unit installed in the water bath. One hour was allowed for temperature equilibration whereupon the capillary was lowered gently to the bottom of the main chamber. The system was allowed to stand undisturbed for about five days, the capillary was removed, the contents were washed into vials containing the scintillator fluid, and the samples were counted.

Results and Discussion

Rate of Deposition

The solubility of Ag_2O in 10 VF KOH at 25°, measured by the tracer method, was found to be 3.5×10^{-4} VF. This compares quite favorably with values obtained polarographically[13]. Equilibrium was reached within a few hours and little, if any, further change was observed in three weeks.

Removal of Ag(I) from the solution by reaction with zinc is shown in Table 19. The results are quantitatively erratic, but some factors appear. The silver was reduced fairly rapidly in the first few hours with at least 90% of the reaction occurring within 5 or 6 hours. There is some indication that the silver concentration leveled off around $1\text{-}2 \times 10^{-6}$ VF with no further reaction occurring.

Diffusion of Ag(I)

Diffusion coefficients were calculated using equations (3) and (4):

$$\gamma = (8/\pi^2)\exp(-\theta) \tag{3}$$

$$\theta = (\pi^2 D\lambda)/4\ 1^2 \tag{4}$$

Table 19

Removal of Silver from KOH Solution by Deposition on Zinc

Weight of Zn (g)	Deposition Time (hours)	Silver Concentration (VF x 10^6)
0.4049	0	340
	4	15
	6	5
	9	5
	29	1
0.3678	0	346
	2	104
	5	33
	7	11
0.4059	0	343
	4	27
	6	12
	28	7
0.3719	0	360
	2	70
	4	32
	6	32

γ = fraction of the original activity remaining in the diffusion cell

D = diffusion constant for the Ag(I) species

λ = diffusion time in seconds

l = length of the diffusion cell in cm.

The average value of D for six runs was 2.75×10^{-6} $cm^2 sec^{-1}$. As was mentioned earlier, this is probably a composite of values for several different silver species. The value for silver ion[15] at infinite dilution is 1.65×10^{-5} $cm^2 sec^{-1}$. If the Stokes-Einstein relation

$$D = RT/6\pi\eta rK \tag{5}$$

is applied to the KOH system, using the measured value of η = 3.6 cp, the value in water is calculated to be about $1.0 \times 10^{-5} cm^2 sec^{-1}$. This suggests that r, the particle radius is larger than that of the relatively simple silver ion in water. Although the assumptions used in this calculation are questionable, the results support the complex-ion hypothesis.

Effect of silver deposit on electrode behavior

Chronopotentiometric evidence indicates that deposition of silver permanently decreases the effective surface area of a zinc-plate anode. The Sand equation[16]

$$i\tau^{\frac{1}{2}} = \tfrac{1}{2}(\pi^{\frac{1}{2}} nFD^{\frac{1}{2}} AC) \tag{6}$$

indicates that $i\tau^{\frac{1}{2}}$ should be constant for linear diffusion to a plane electrode of fixed area if the bulk concentration of electroactive material is constant. Delahay, Mattax, and Berzins[17] showed that the transition time in the anodic dissolution of metals is controlled by the concentration of the complexing substance. Thus, one would expect the transition time for the dissolution of zinc to be controlled by the hydroxide concentration. However, relatively non-porous films on the electrode surface may tend to prevent diffusion of active material to reactive sites causing a change of

$i\tau^{\frac{1}{2}}$ for the system. Something of this sort appears to occur in the system under study.

Table 20

Chronopotentiometric Behavior of Zinc Anodes Plated with Silver

Current Density (mA/cm^2)	Transition Time (sec)	$i\tau^{\frac{1}{2}}$ ($mA\text{-}sec^{\frac{1}{2}}/cm^2$)
150	47.7	1059
125	68.3	1032
100	119	1091
	Average	1044
Untreated Zn		
150	65.7	1214

Table 20 shows the effect on $i\tau^{\frac{1}{2}}$ in 10 VF KOH of deposition of silver on the zinc-sheet electrodes. The plates were immersed for several days in KOH solutions saturated with Ag_2O. The plates were then transferred to 10 VF KOH solutions and the chronopotentiograms made. The average $i\tau^{\frac{1}{2}}$ of 1.04×10^3 $mA\text{-}sec^{\frac{1}{2}}/cm^2$ is significantly lower than the 1.21×10^3 $mA\text{-}sec^{\frac{1}{2}}/cm^2$ value found when the zinc had not been exposed to Ag(I).

The values reported are averages with the first few eliminated. In general, the first run on a treated plate gave $i\tau^{\frac{1}{2}}$ about 750 $mA\text{-}sec^{\frac{1}{2}}/cm^2$; the second gave value close to the average. If one assumes that plated silver decreases the effective surface area, then that area is initially about 62% of the normal. Evidently, much of this film is removed, probably by gas formation, as the transition time is passed. However, the material that remains adheres strongly (or the surface of the zinc is permanently and reproducibly altered) so that the effective area remains about 86% of the normal value.

20

Table 21 shows the results of chronopotentiograms made in 10 VF KOH saturated with Ag_2O but without prior deposition of silver on the zinc.

Table 21

Chronopotentiometric Behavior of Zinc Anodes Without Prior Exposure to Ag(I)

i (mA/cm^2)	$i\tau^{1/2}$ ($mA\text{-}sec^{1/2}/cm^2$)
150	995 ± 34
125	1070 ± 62
100	1133 ± 76

Here, a drift in $i\tau^{1/2}$ can be seen which was not observed previously. The meaning is not clear. Certainly, the concurrent chemical and electrochemical oxidation of the zinc will affect the kinetic parameters for the system. More work is necessary to evaluate this condition.

A series of experiments was made with plated electrodes as before except that current was continued after the transition time was passed; gassing was permitted for 36 seconds. Subsequent chronopotentiograms showed transition times almost the same as those found for untreated electrodes. This observation supports the argument that a significant portion of the silver layer is loosely held and that vigorous action such as gassing will remove most of the remaining deposit.

It must be concluded from this work that Ag(I) diffuses rapidly to the zinc electrode through a KOH solution and that silver is rapidly plated out. The plated metal does not adhere strongly for the most part, but that which does decreases the effective anode area by at least 10-15%; only drastic action will remove this residue. Consequently, it is most important that no silver species be allowed access to the zinc electrode in a silver-zinc cell.

C. HYDROGEN OVERVOLTAGE ON ZINC

Introduction

Hydrogen overvoltage has been studied on many metals, but most of the work has been done in acid or neutral solutions. A few investigations such as those by Makrides[18], Weininger and Breiter[19], and Ohmuri and Matsuda[20] have been done on nickel in dilute alkaline solutions. Nothing in the recent literature indicates any similar study on zinc or cadmium, particularly at high alkali concentrations. Since hydrogen is evolved on zinc and cadmium electrodes on overcharge, such studies seem important.

Only some preliminary work is reported here. Project redirection caused this portion of the work to be discontinued before much useful information could be gathered. A few interesting trends were noted which might lead to further investigation at a later time.

Experimental

Reagent grade chemicals were used without further purification. Zinc, both sheet and wire, was grade 6N. Water was triply distilled, the last distillation being from alkaline permanganate.

The cells were of a simple, multi-compartment construction. A "buffer" compartment containing a solution identical to that in the working compartment was placed between the reference electrode and the working compartment. A similar "buffer" was placed between the auxiliary and working electrodes when the auxiliary was mercury. A Luggin capillary was placed within a few millimeters of the working electrode. Provision was made for bubbling either H_2 or N_2 through the solution. The reference was a Hg/HgO electrode.

The working electrode potential was set with a Wenking Model 66 TS-1 potentiostat. A precision resistor was placed in the auxiliary electrode

lead and the current determined by measuring the IR drop with a Leeds and Northrup K-3 potentiometer.

Wire, wire-end, and plate working electrodes were tried. These were mounted in various orientations from horizontal through vertical. Concentrations of KOH ranged from 0.1 VF to 10 VF.

Electrodes were pre-treated by cathodic electrolysis at 5 mA for at least 15 minutes. The solutions were swept with N_2 and usually, but not always, saturated with H_2 by slowly bubbling the purified gas through the system. Purification was accomplished by passing the gas through a vanadous solution[5]. The flowing gas also provided stirring. Oxygen was excluded at all times.

Results and Discussion

Results were not generally reproducible. It is probable that much greater care must be exercised in purification of reagents and in pretreatment of electrodes. Nevertheless, some generalized trends are shown. Data given here are for wire working electrodes oriented vertically. The Luggin capillary was positioned at one side with its tip within 1 mm of the wire.

Figure 14 shows representative plots of log i vs polarization. The term "polarization" will be used in accordance with the arguments presented by Vetter[21]. In most cases, a "Tafel region" was observed and extrapolation of this to zero polarization was used to determine the "extrapolated exchange current-density", i_o.

Although scatter was severe, an increasing i_o was found with increasing KOH concentration. Thus, i_o at 0.1 VF KOH is probably 10-20 $\mu A/cm^2$; at 1 VF KOH, 50-75 $\mu A/cm^2$; at 10 VF KOH, 150-250 $\mu A/cm^2$. Matsuda and Notoya[22] suggest a concentration-exchange current relationship for H_2 evolution of

$$i_o = K(C^{Na^+})^{\frac{1}{2}} \qquad (7)$$

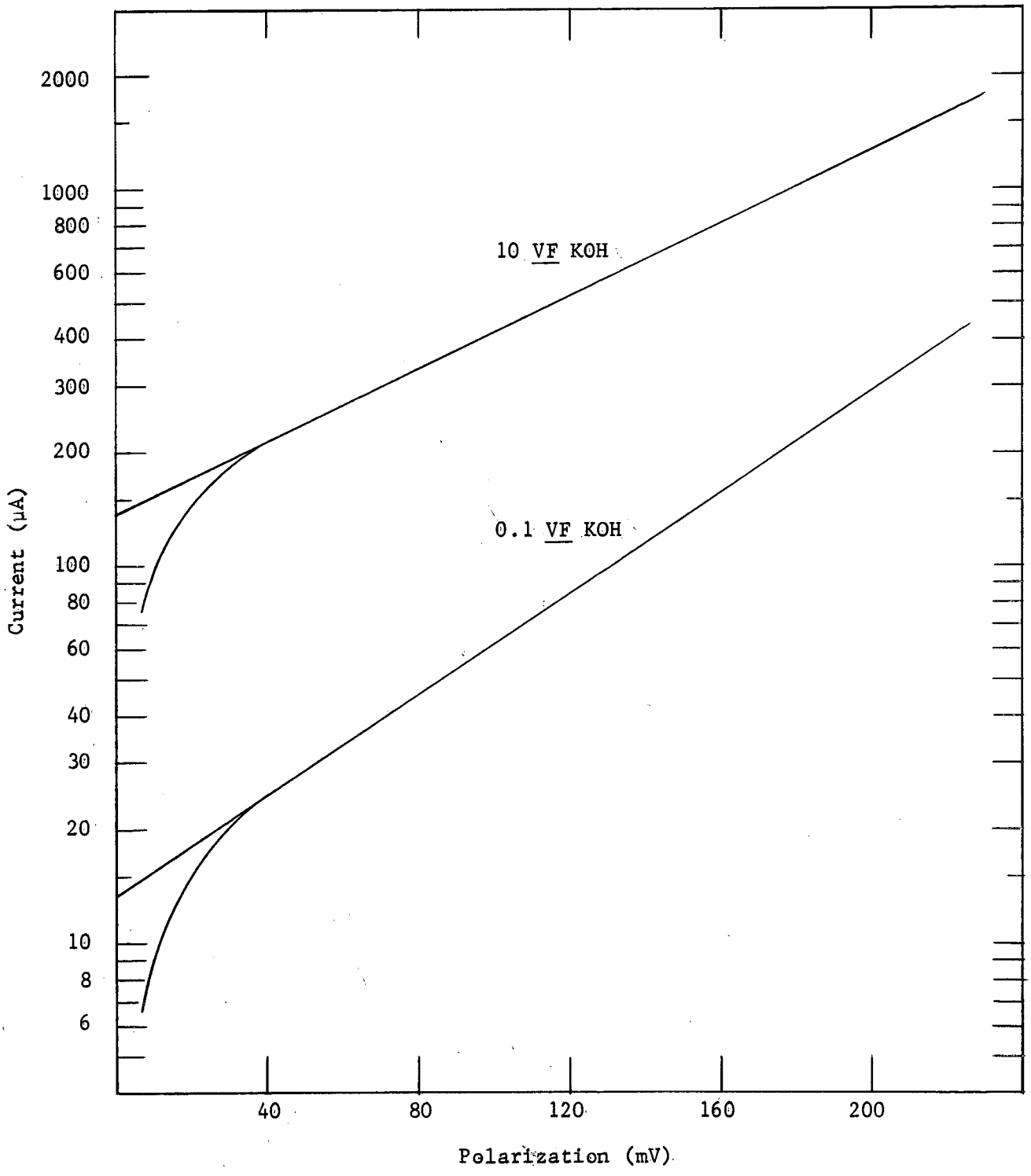

Figure 14. Hydrogen Polarization of Zinc Electrode

on platinum and Ohmuri and Matsuda[20] suggest a similar relationship on nickel. It is possible that this relationship also holds for the Zn-KOH system, although one would expect much greater activity effects. Ohmuri and Matsuda also observed that a change in concentration of Na^+ merely shifted the Tafel line but did not change its slope. The shift at a given current-density was about 65 mV for a 10-fold change in concentration. Figure 14 shows a change in slope with concentration but the shift with concentration is in the right range (130 mV) for a 100-fold concentration difference. These qualitative estimates suggest that the general mechanisms involved for H_2 formation on zinc are quite similar to those found on nickel.

A single experiment using a cadmium wire electrode in 10 VF KOH produced a fairly good Tafel line which extrapolated to give i_o = 12 mA/cm^2. This is a very high value and suggests a very low hydrogen overvoltage for cadmium.

In general, the tentative results indicate a lowering hydrogen overpotential with increasing KOH concentration, possibly following a square-root relationship. The implication is that gassing during overcharge in 10 VF KOH electrolyte solutions will occur fairly readily on zinc electrodes and very readily on cadmium. A great deal more work must be done on these rather complicated systems before any reasonable understanding can be expected.

D. THERMAL DECOMPOSITION OF AgO AND Ag_2O

Introduction

Argentic oxide is thermally decomposed in two steps, these being described by the equations

$$4\ AgO \xrightarrow{\Delta} 2\ Ag_2O + O_2 \qquad (8)$$

$$2\ Ag_2O \xrightarrow{\Delta} 4\ Ag + O_2 \qquad (9)$$

Nagy, Moroz, and Casey[23] indicate that reaction (8) is slow but finite at temperatures as low as 100°. Work in this laboratory[1] has shown that AgO is 50% converted to Ag_2O within 24 hours at about 120°. These data suggest that thermal sterilization of dry, fully-charged silver electrodes is not feasible.

Evidence will be presented to show that reaction (8) slows greatly as the amount of AgO decreases and that reaction (9) occurs to some small extent before reaction (8) is complete. Thus, the use of thermal decomposition curves for determining kinetic parameters or as an analytical tool for this system becomes questionable.

The very low temperatures at which AgO decomposes raises a question about its behavior below 100° over extended time periods. Work described in this report will show that, although there is no indication of actual decomposition below 90°, physical changes apparently occur which may well affect its heterogeneous reactivity.

Experimental

The general arrangement of equipment has been described previously[1]. The balance was mounted in a Cahn #2005 Glass Vacuum Bottle. The hangdown tube was attached to the bottle through a T/S 40/35 joint. The inner thermocouple was attached through a T/S 10/30 joint. The sample was heated in a Lindberg Type 123-2 8" split-tube furnace. Temperature was controlled with a F & M Model 240M temperature controller. The control thermocouple was cemented to the ceramic tube of the furnace outside of the hangdown tube. The temperature inside the tube at the sample position was recorded with a Texas Instruments Servo/Riter Model II 1-mV recorder operated through a Cahn Recorder Controller. Several layers of sheet aluminum were placed on top of the furnace to shield the balance from furnace heat. The hangdown tube and all port caps were coated with platinum and grounded to prevent build up of static charge.

Figure 15 shows a schematic diagram of the total system where atmospheric control was required. For vacuum work, the system was pumped continuously to maintain a pressure less than 1 torr. Where a specific atmosphere was desired, the system was evacuated, the desired gas let in, the system evacuated again, and the entire flushing procedure repeated several times. The system was then maintained at about 2 torr above atmospheric. In this way, moisture should have been excluded from the system. Laboratory air was admitted by means of a Planchet vibratory pump through a Kontes K-627940 flow regulator.

Results and Discussion

Activation energies for the decomposition of Ames AgO and its product, Ag_2O, were estimated from thermograms run at 2°/min, 5°/min, and 10°/min. Data were treated according to the method of Flynn and Wall[24] and Doyle[25]. Calculated activation energies were 26.2 kcal/mole for AgO and 43 kcal/mole for Ag_2O. Although the thermograms were interrupted for several hours between 250° and 300° to allow complete decomposition of AgO, later work, shown below, raises questions about the method.

Figure 16 shows the behavior of a sample of Ames AgO heated sequentially at three different temperatures. At 160°, the behavior is as expected. On raising the temperature to 270°, a slight increase in decomposition is observed. At 287°, the weight decreased below that expected for complete decomposition of AgO to Ag_2O and continued to decrease. Furthermore, the rate of reaction seemed to increase with time.

Figure 17 shows the behavior of K & K Ag_2O heated sequentially at different constant temperatures. In the time allowed, no loss (other than initial moisture) was observed up to 270°. At 290°, the phenomenon observed in the Ames sample was again seen with the increased rate with time.

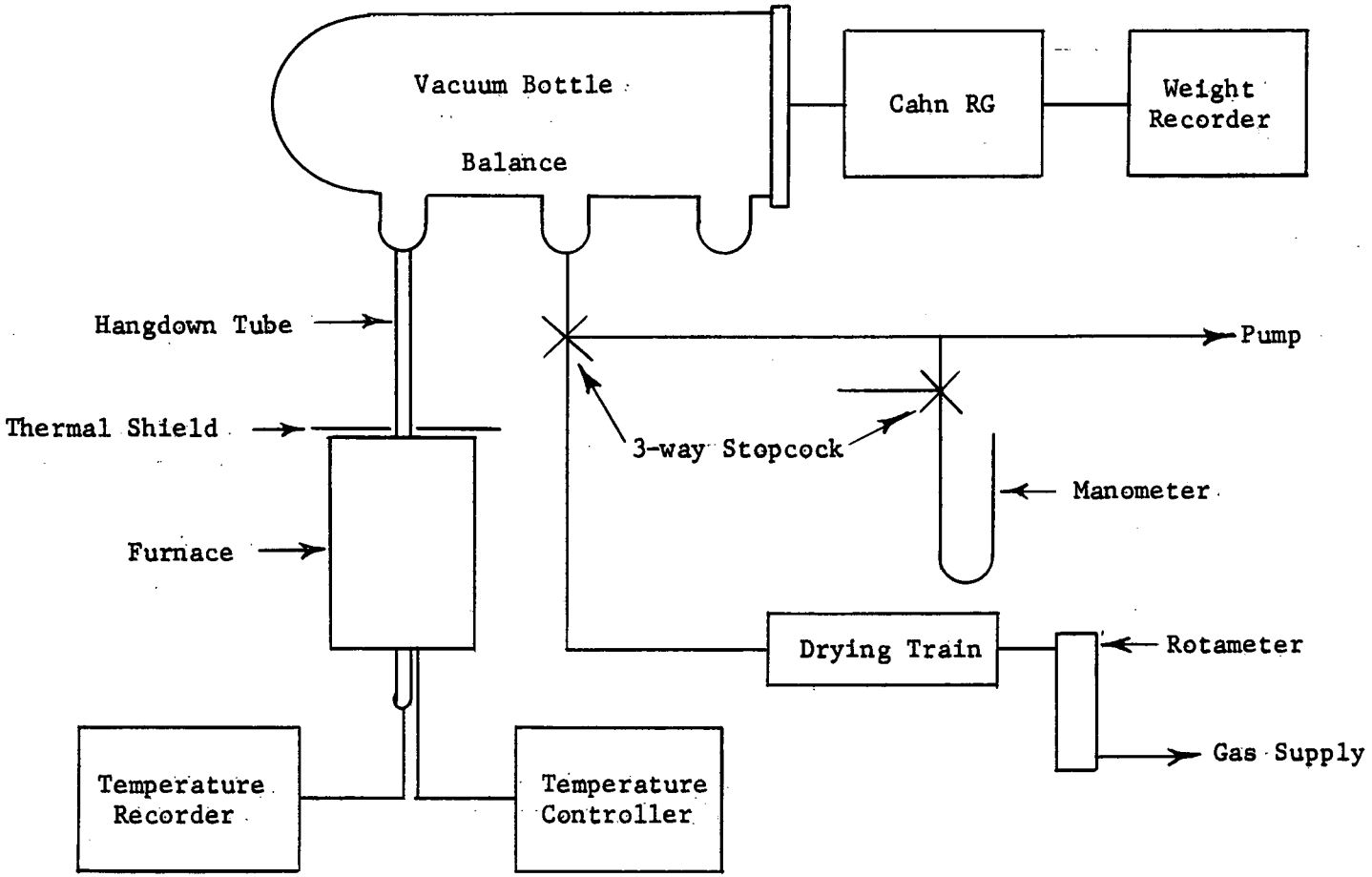

Figure 15. Schematic of Thermogravimetric System

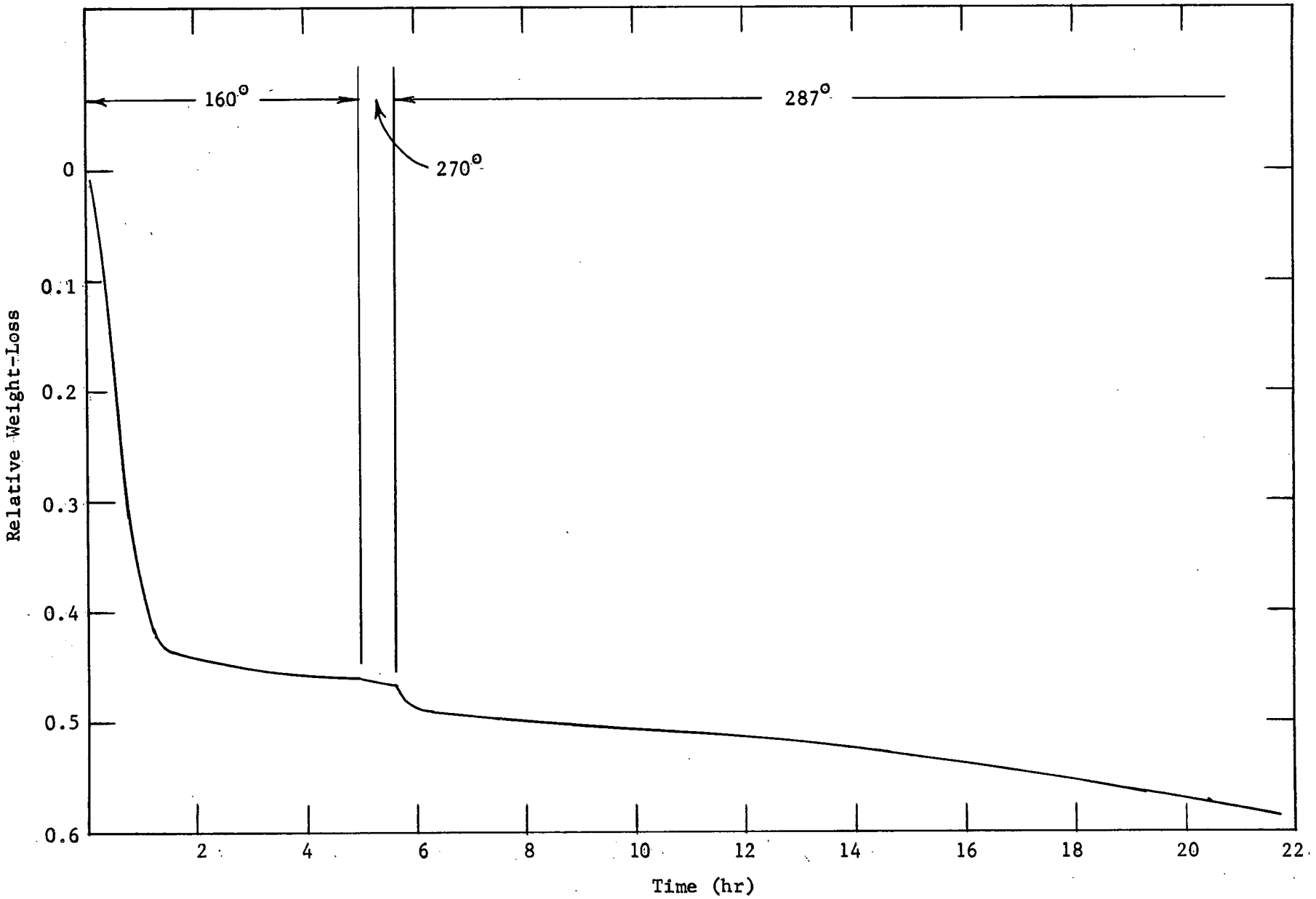

Figure 16. "Constant-Temperature" Thermogram of Ames AgO

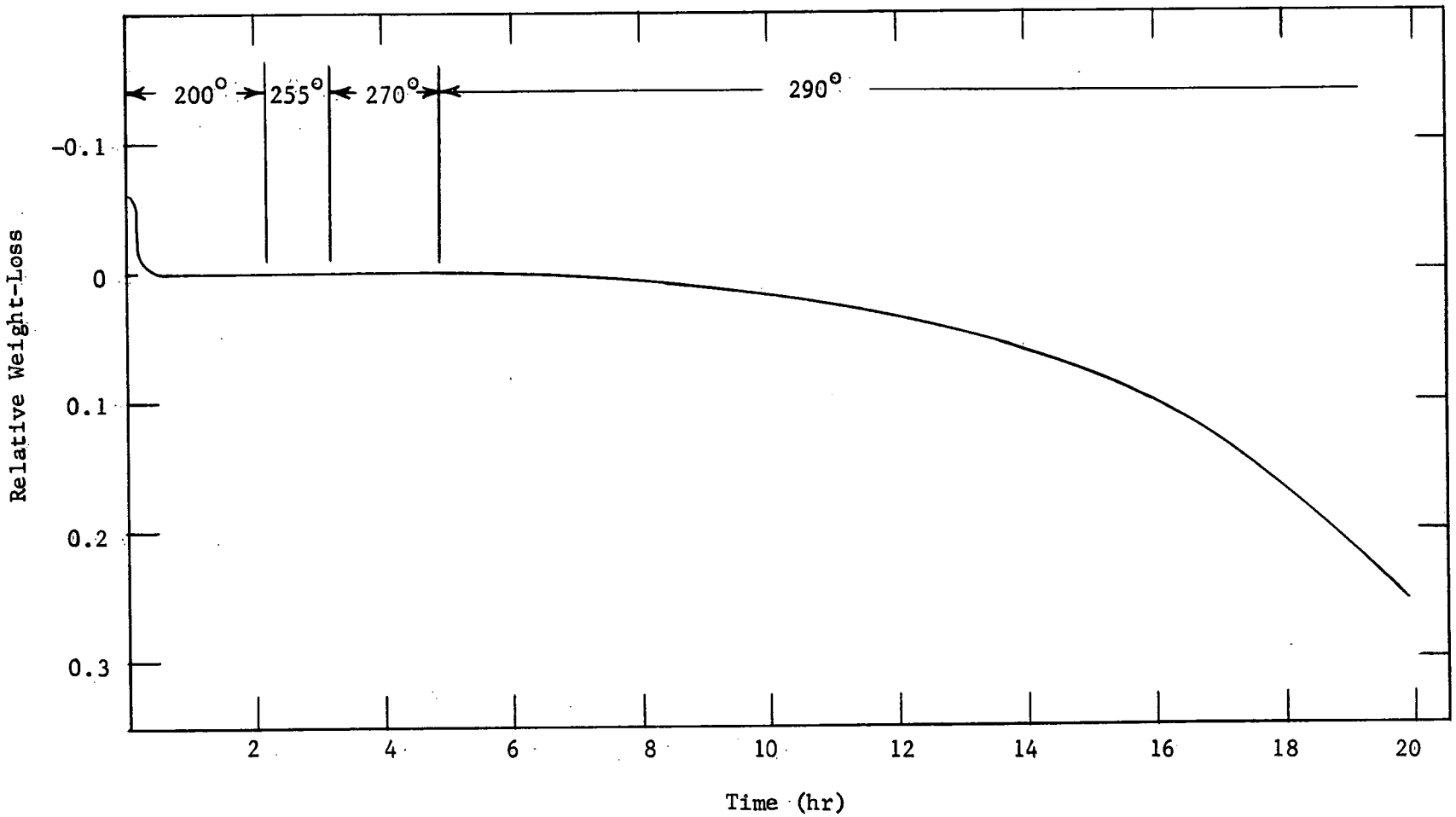

Figure 17. "Constant-Temperature" Thermogram of K & K Ag_2O

These phenomena were not expected. Particularly, the increasing rate with time was surprising. Normally, one would expect the reverse. Silver metal appears to form on the surface and work inward; this should also cause a rate decrease. However, results of subsequent work at low temperatures suggest changes in the characteristics of Ag_2O on heating. The exact nature of these changes is not known, but they probably increase the effective surface area of the material. Changes in crystal structure may be possible, also. This heating effect may occur more rapidly at the higher temperatures allowing a more rapid decomposition as the process proceeds.

It is necessary to know the dry, room-temperature weight of a sample if a reliable analysis of that substance is to be made. There was some indication that a relatively simple analysis of AgO-Ag_2O mixtures was possible by stepwise thermal decomposition. The method would be long, but many samples could be run simultaneously in furnaces at appropriate temperatures if the decompositions could be accomplished in a laboratory atmosphere. Initial attempts showed serious relative errors, in some cases exceeding 10%. Furthermore, samples dried at 100° and cooled over calcium chloride in a desiccator seemed to show a continuous weight-gain over several days. These observations led to a series of experiments to determine the thermal behavior at temperatures below 100°.

An experiment was performed with the thermobalance on a sample of Ames AgO in the laboratory atmosphere. The sample was alternately heated at a fixed temperature for some period and then held at room temperature. The results are shown in Figure 18. Each heating segment was continued until the weight had decreased to about 24.62 mg; each room-temperature segment was held until the rate of increase, if any, was very small.

The startling result from this experiment is the gain in weight over the initial weight after each heating. It is also remarkable that the

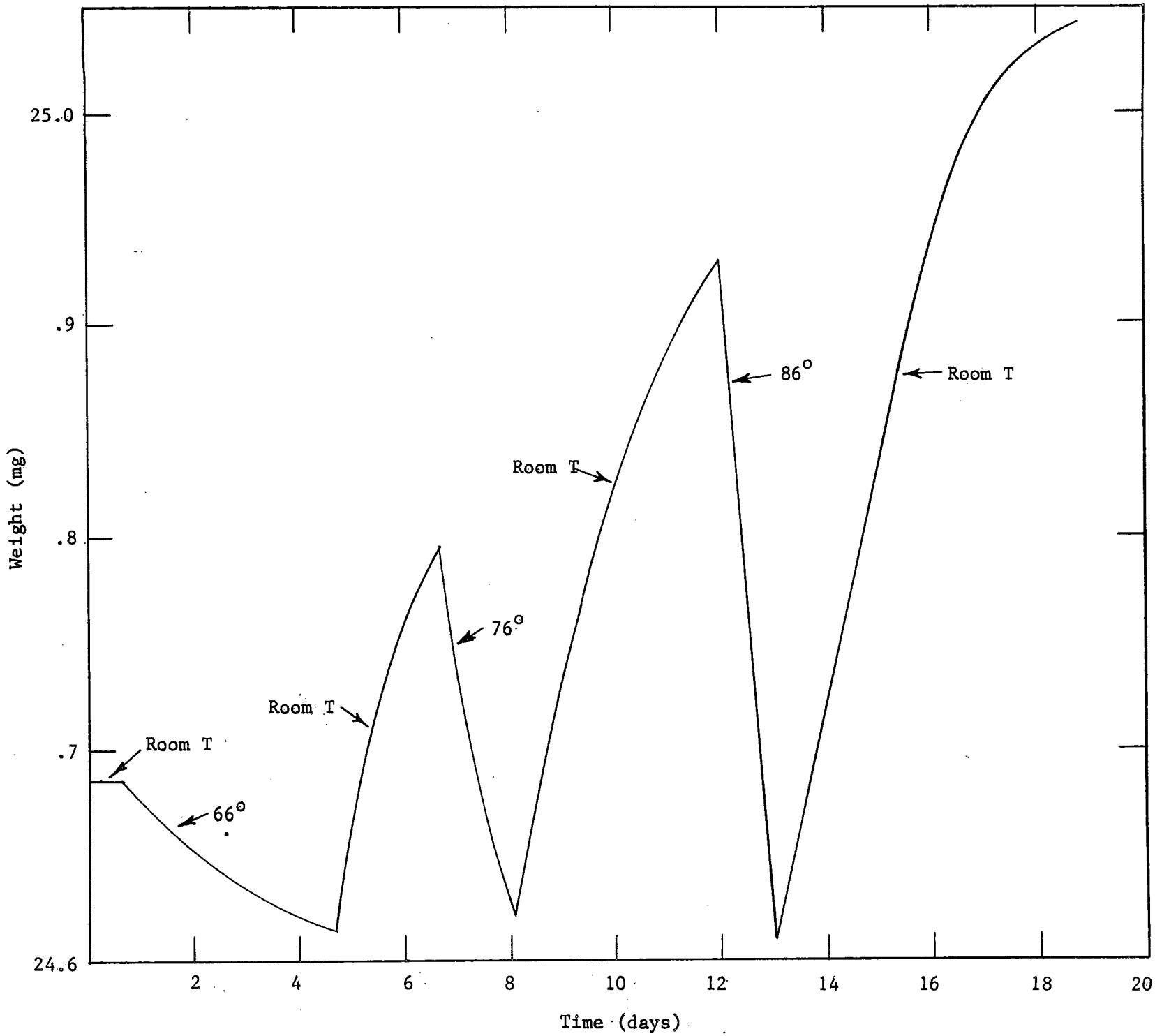

Figure 18. Adsorption and Desorption on AgO

gain increased after each heating so that the final weight was 1.4% higher than the initial.

The variation in weight-gain observed above might have been the result of repeated heating or of heating at different temperatures. Two experiments were performed in which each heating segment was held at 65°. The results of the first experiments are shown in Table 22. In this case, each segment was continued until constant weight was attained. The results of the second experiment are shown in Figure 19. Here, heating segments were continued for rather arbitrary periods ranging from 3.4 to 24.6 hours. The first four heating periods were less than 24 hours, the rest were about 24 hours.

In both experiments, repeated heating at 65° caused a net gain in weight on cooling (referred to the initial weight). Furthermore, this gain increased with the number of cycles in an almost linear fashion. It is possible that, had all the heating segments been of equal length, the linearity would have been better.

Ames AgO was thermally reduced to Ag_2O by heating at about 250° and was then returned to room temperature. The resulting weight-gain is shown in Figure 20. In fact, this is not surprising if the observed results were caused by adsorption. Figure 21 shows the results of allowing K & K Ag_2O to stand at room temperature <u>without prior heating</u>. This material had been stored in a bottle over several years with samples being removed at various times. There was ample opportunity for the material to adsorb gases from the laboratory air. Yet, at room temperature on the thermal balance, this material behaved in much the same way as Ag_2O which had been freshly prepared by thermal decomposition.

Similar experiments were run below 100° using aluminum weights and with pure silver powder having a mean particle size of 1.45 micron (Ames

Table 22

Adsorption and Desorption of Gas on AgO

Temperature was held at about 65° during the heating segment of the cycle and at room temperature during the rest of the cycle. Each segment was continued until constant weight was attained. Gain and loss is expressed with reference to the initial weight at room temperature.

Segment	Gain(γ)	Loss(γ)
1st heat		25
1st cool	55	
2nd heat		105*
2nd cool	160	

*Constant weight was not attained.

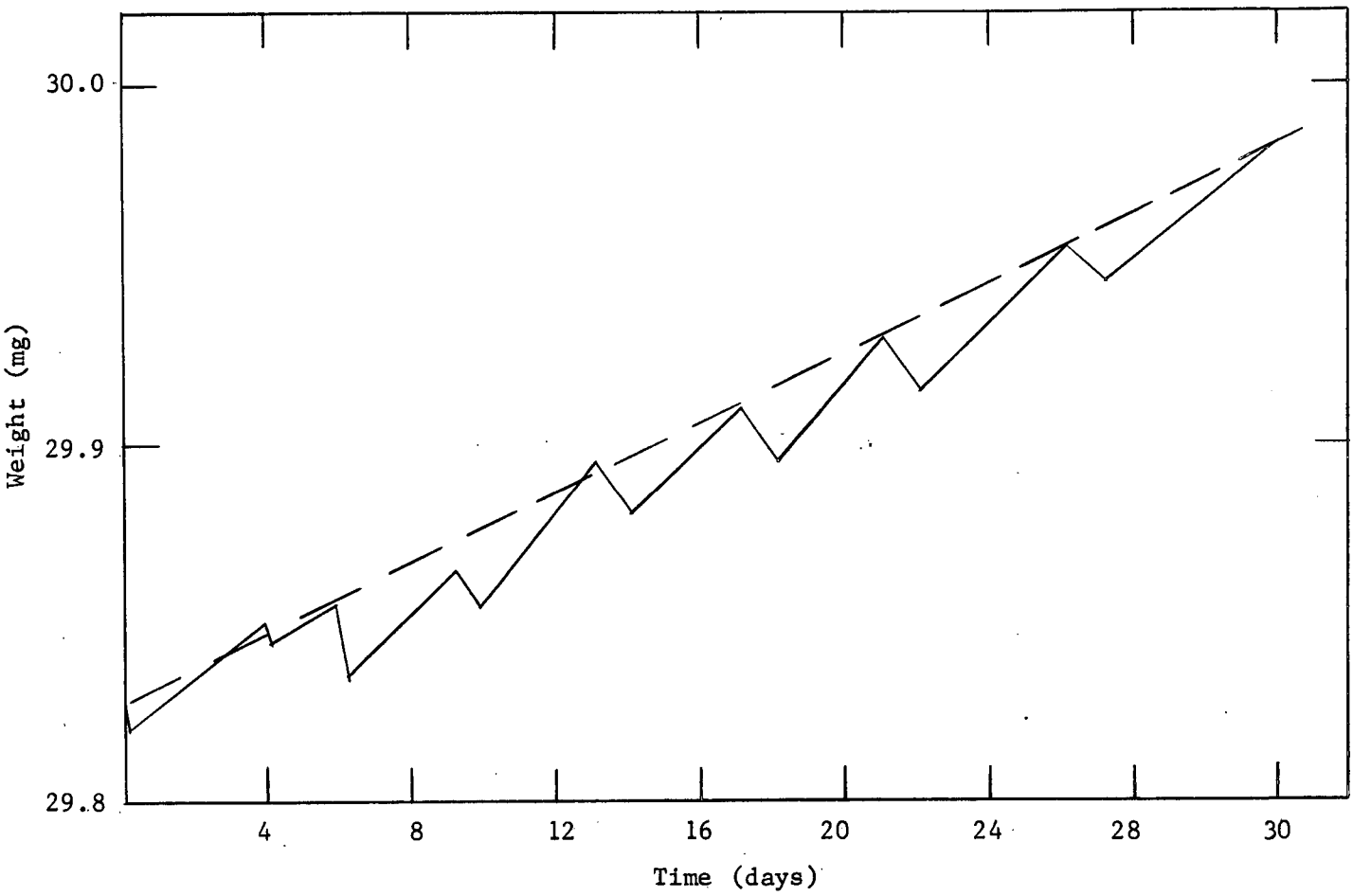

Figure 19. Effect of Thermal Cycling on Weight of AgO

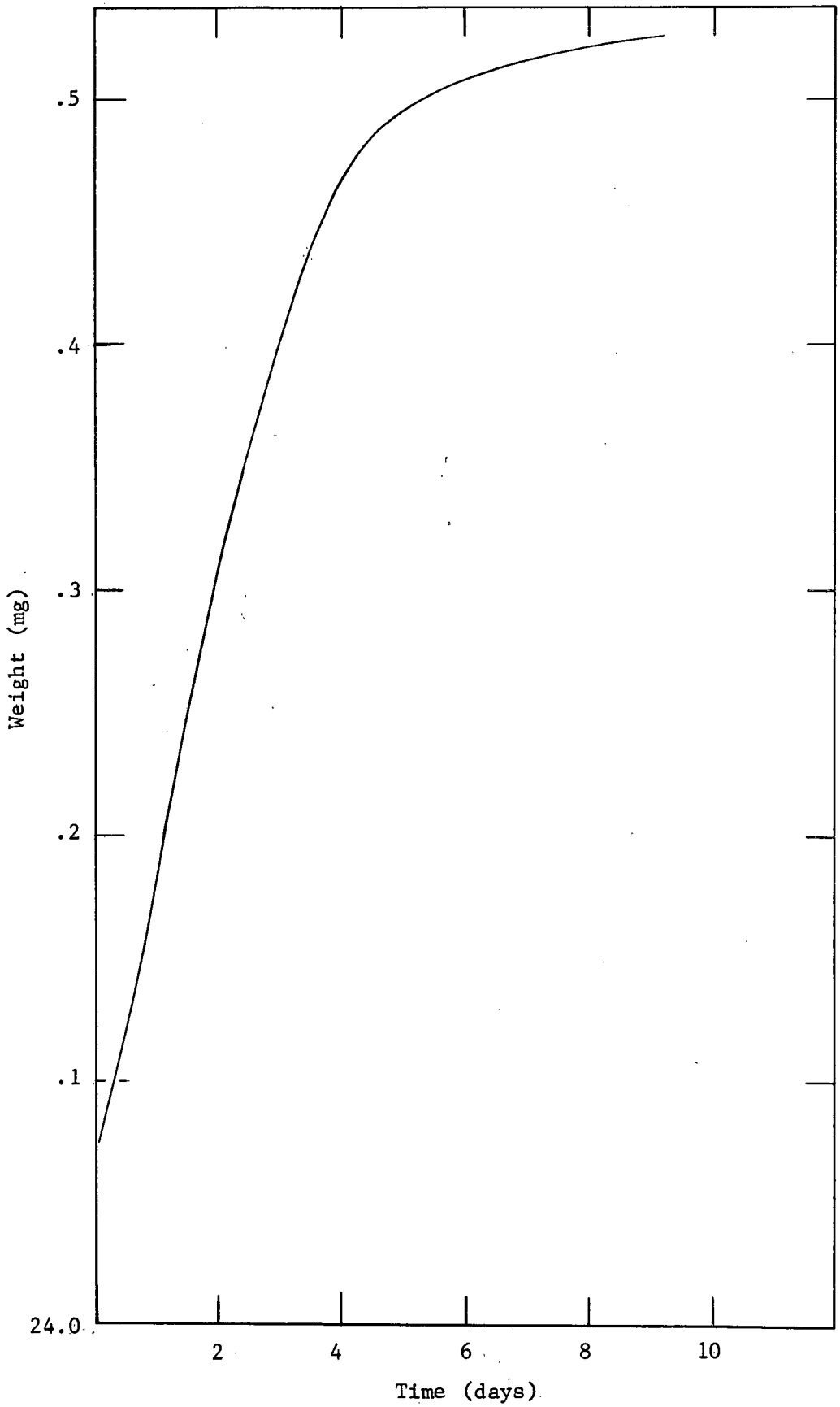

Figure 20. Adsorption on Ag_2O

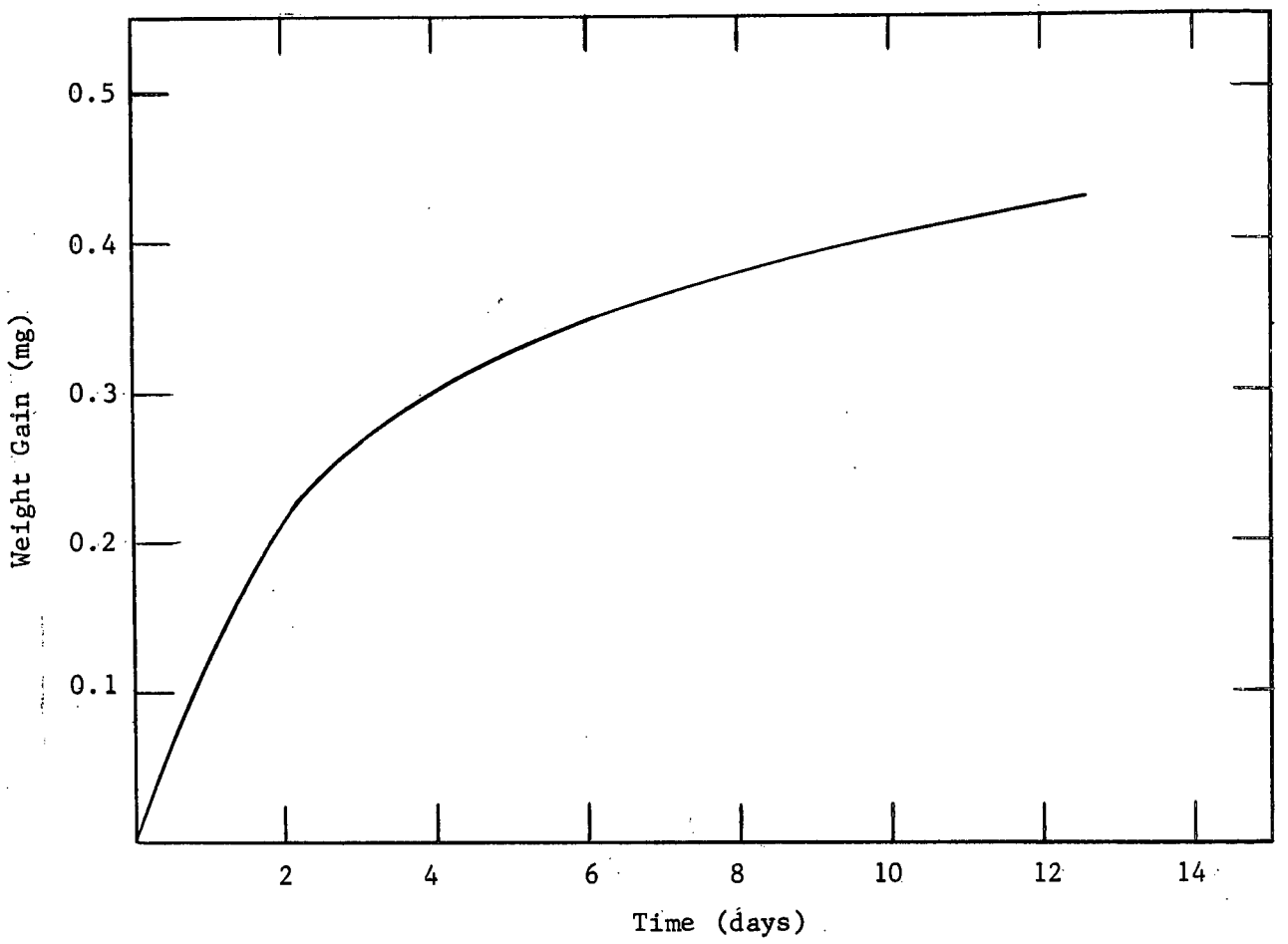

Figure 21. Adsorption of Gas by Ag_2O at Room Temperature

Chemical Works Type SG; 99.9+ purity). Except for a slight initial moisture loss on heating the powder, no weight changes were observed. Thus, the phenomena are evidently characteristic of AgO and Ag_2O.

One can assume that the weight-gains are the result of adsorption of one or more components from the atmosphere. One can further assume that AgO must be thermally "activated" before significant adsorption will occur. Now, certain facts emerge. First, no apparent "activation" occurs below about 60°. Secondly, if the material is "activated" at 65° for several hours, adsorption at room temperature will exceed the initial desorption. Thirdly, reheating will not remove all of the adsorbed material unless the heating period is much longer than that first used or unless the temperature is higher. There may be crystal re-orientation occurring which allows a tight bonding of adsorbed molecules so that considerable energy is required to remove them. Further heating may merely increase the extent of this re-orientation with the result that an overall increase of weight is observed with time. Alternatively, the process may simply be an increase in effective surface area as heating is continued. One might argue that this also is a crystal re-orientation, but it would be limited to the surface structure.

No explanation is offered for the behavior of Ag_2O. Certainly, saturation appears to occur after about two weeks. Yet the fact that "old" material behaves in much the same way as freshly prepared Ag_2O is curious. Much more work is needed here.

None of the above indicates what component of the atmosphere was being adsorbed. Therefore, several experiments were performed in which the samples were kept in controlled atmospheres. All heating was done at 62-67°.

A 28-mg sample of AgO was heated in vacuum for three days and lost 120 γ. On returning the sample to room temperature, it lost another 10 γ in two days. Laboratory air was admitted after which no weight change was observed over a period of seven hours. The sample was again heated for three days in the laboratory atmosphere and lost 45 γ. Left at room temperature, for five days, it gained 105 γ.

This experiment suggests that "activation" occurs only in the atmosphere since the usual decrease followed by an increase did not occur when the system was heated in vacuum and left cold in air.

Another sample was heated in dry N_2 for five days and lost 95 γ. The sample-weight did not change on standing in dry N_2 at room temperature for two days. Thus, either "activation" and/or adsorption did not occur in this atmosphere.

A sample heated in dry O_2 for five days lost 70 γ and did not change in dry O_2 at room temperature over a two-day period. However, when the O_2 flow was stopped, the sample began to gain weight immediately for a total increase of 140 γ over five days. When O_2 flow was started again at any time during the period, weight-change ceased within an hour and resumed again as soon as the flow was stopped. The only explanation seems to be that moisture was leaking into the system when flow was stopped; since the joint nearest the sample is about 10 cm away, transport of water through the joint and to the sample seems remarkably rapid.

The water hypothesis does not correlate with the results in vacuum reported above unless the presence of O_2 is necessary to bring about "activation". Or O_2 may somehow catalyze the adsorption of water or vice versa.

When a sample was heated in dry air, it lost only 30 γ in five days. On standing at room temperature in dry air, it gained only 40 γ in three days. Both changes were lower than expected. Flow was not stopped as in

the pure-oxygen experiment so no comparison can be made with that observation.

No very satisfactory explanation can be advanced for the above observations at this time. That some sort of interaction occurs between one or more components of the atmosphere and both of the oxides of silver seem obvious. A simple surface adsorption is possible but does not seem likely. The thermal "activation" which appears to occur is quite evidently dependent on the sample environment, particularly on the presence of water and/or oxygen.

Suggested Work

The behavior of the system in vacuum suggests that an analytical procedure may yet be feasible provided that the reaction is carried out in the absence of any atmosphere. This would be tedious, of course, but may be better than any available wet method. This possibility should be investigated.

Considerably more work should be done to elucidate the adsorption mechanism. Considerable information can be obtained before investigating structural changes by X-ray methods. If oxygen is being adsorbed as the predominant species, then serious consequences are suggested if dry-charged silver electrodes are exposed to moderately elevated temperatures (e.g., summer desert) for extended periods. The possibility of subsequent gas evolution has already been suggested by Butler[26].

REFERENCES

[1]G. M. Arcand, "The Reactions Pertaining to Zinc-Silver and Cadmium-Silver Batteries," August 1, 1968, Final Report on Contract JPL 951887.

[2]"Alkaline secondary cell with an amalgam anode involving a liquid phase." Mallory Batteries, Ltd. Neth. Appl. 6.400.259(Cl. H01m) July 17, 1964 U. S. Appl. Jan. 16, 1963.

[3]J. A. Le Duc, J. G. Kourilo, and C. Lurie, J. Electrochem. Soc. 116, 546(1969).

[4]S. Lica, Rev. Chim.(Bucharest) 20, 609(1969). CA 73, 9983n(1970).

[5]L. Meites, "Polarographic Techniques," 2nd ed., Interscience Publishers Inc., New York, N.Y., 1965, p.88.

[6]J. J. Lingane, "Electroanalytical Chemistry," Interscience Publishers, Inc., New York, N.Y., 2nd ed., 1958, p.452.

[7]E. C. Potter, "Electrochemistry," The MacMillan Co., New York, N.Y., 1956, p. 17.

[8]W. M. Latimer, "The Oxidation States of the Elements and their Potentials in Aqueous Solutions," Prentice-Hall, Inc., New York, N.Y., 1938.

[9]F. A. Cotton and G. Wilkinson, "Advanced Inorganic Chemistry," 2nd. ed., Interscience Publishers, Inc., New York, N.Y., 1966, p. 482.

[10]T. P. Dirkse, L. A. Vander Lugt, and H. Schnyders, J. Inorg. Nucl. Chem. 25, 859(1963).

[11]G. Biedermann and L. G. Sillen, Acta Chem. Scand. 14, 717(1960).

[12]R. F. Amlie and P. Ruetschi, J. Electrochem. Soc. 108, 813(1961).

[13]Y. Israel and A. Vroman, Anal. Chem. 31, 1470(1959).

[14]J. S. Anderson and K. Saddington, J. Chem. Soc. 1949, S381.

[15]L. Meites, "Polarographic Techniques," 2nd. ed., Interscience Publishers, Inc., New York, N.Y., 1965, p. 144.

[16]Ibid., p. 556.

[17]P. Delahay, C. C. Mattax, and T. Berzins, J. Am. Chem. Soc. 76, 5322(1954).

[18]A. C. Makrides, J. Electrochem. Soc. 109, 977(1962).

[19]J. L. Weininger and M. W. Breiter, J. Electrochem. Soc. 111, 707(1964).

[20]T. Ohmuri and A. Matsuda, J. Res. Inst. Catal., Hokkaido Univ. 17, 39(1968).

[21]K. J. Vetter, "Electrochemical Kinetics: Theoretical Aspects," Academic Press, New York, N.Y., 1967, p. 9.

[22]A. Matsuda and R. Notoya, J. Res. Inst. Catal., Hokkaido Univ. 14, 165(1966).

[23]G. D. Nagy, W. J. Moroz, and E. J. Casey, Proc. Ann. Power Sources Conf. 19, 80(1965).

[24]J. H. Flynn and L. A. Wall, Polymer Lett. 4, 323(1966).

[25]C. D. Doyle, J. Appl. Polymer Sci. 5, 285(1961).

[26]E. A. Butler, JPL Tech. Rept. No. 32-535, December 22, 1963.